Hindawi Publishing Corporation
Journal of Sensors
Volume 2012, Article ID 598178, 21 pages
doi:10.1155/2012/598178

Review Article

Photonic Crystal Fibers for Sensing Applications

Ana M. R. Pinto and Manuel Lopez-Amo

Departamento de Ingeniería Eléctrica y Electrónica, Universidad Pública de Navarra, Campus de Arrosadía, Navarra 31006 Pamplona, Spain

Correspondence should be addressed to Ana M. R. Pinto, anamargarida.rodrigues@unavarra.es

Received 5 December 2011; Accepted 2 February 2012

Academic Editor: Wolfgang Ecke

Photonic crystal fibers are a kind of fiber optics that present a diversity of new and improved features beyond what conventional optical fibers can offer. Due to their unique geometric structure, photonic crystal fibers present special properties and capabilities that lead to an outstanding potential for sensing applications. A review of photonic crystal fiber sensors is presented. Two different groups of sensors are detailed separately: physical and biochemical sensors, based on the sensor measured parameter. Several sensors have been reported until the date, and more are expected to be developed due to the remarkable characteristics such fibers can offer.

1. Introduction

Optical fibers (OFs) development in 1966 revolutionized fields such as telecommunications and sensing, leading to the creation of high sensitivity and controlled systems based on light guidance. The remarkable characteristics of fiber optics such as geometric versatility, increased sensitivity over existing techniques, and inherent compatibility with fiber optic telecommunications technology make them stand out for sensing applications. Optical-fibers-based sensors are low cost and efficient solutions for several industries due to their high sensitivity, small size, robustness, flexibility, and ability for remote monitoring as well as multiplexing. Other advantages entail their aptitude to be used even in the presence of unfavorable environmental conditions such as noise, strong electromagnetic fields, high voltages, nuclear radiation, in explosive or chemically corrosive media, at high temperatures, among others. Even though standard optical fibers present an excellent performance in fiber telecommunications, the intrinsic properties of silica have imposed restrictions in the evolution of this technology. The first evident restriction is the material selection for the core and cladding, in order to have matching thermal, chemical, and optical properties. Other limitations are related to its geometry and refractive index profile, which does not allow for freely engineering optical fiber characteristics such as inherent losses, dispersion, nonlinearity, and birefringence in order to progress in applications such as high power lasers or fiber sensors, among others. These limitations and restrictions have been refined during 30 years of exhaustive research, taking fiber optic technology nearly as far as it could go [1, 2].

The appearance of photonic crystal fibers (PCFs) in 1996 was a breakthrough in fiber optic technology given that these fibers not only had unprecedented properties as they could overcome many limitations intrinsic to standard optical fibers. Photonic crystal fiber geometry is characterized by a periodic arrangement of air holes running along the entire length of the fiber, centered on a solid or hollow core. The major difference between both kinds of fibers relies on the fact that the waveguide properties of photonic crystal fibers are not from spatially varying glass composition, as in conventional optical fiber, but from an arrangement of very tiny and closely spaced air holes which go through the whole length of fiber. In contrast with standard optical fibers, photonic crystal fibers can be made of a single material and have several geometric parameters which can be manipulated offering large flexibility of design. Even more, these fibers offer also the possibility of light guiding in a hollow core, opening new perspectives in fields such as nonlinear fiber optics, fiber lasers, supercontinuum generation, particle

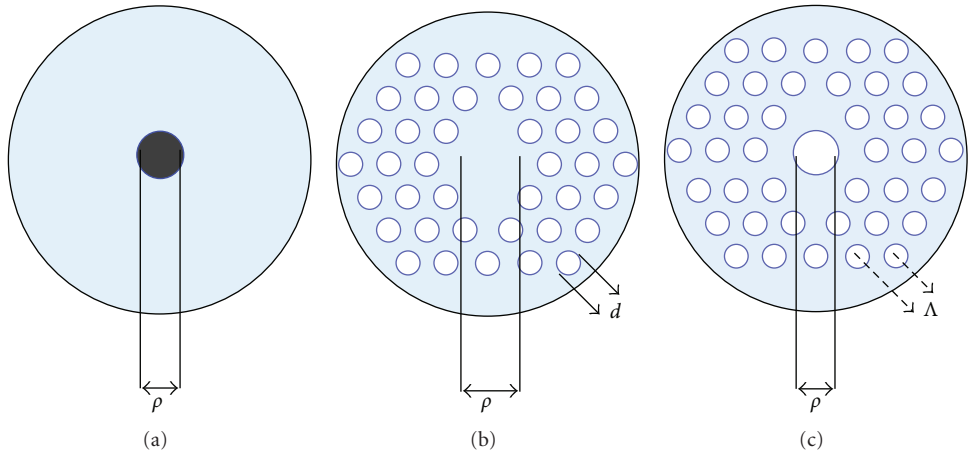

Figure 1: Drawing of the cross-section of (a) SMF, (b) solid core PCF, and (c) hollow-core PCF. Colors: blue: silica, grey: doped silica, white: air.

guidance, and fiber sensors [3, 4]. Therefore, there is a high interest of the scientific community in employing photonic crystal fibers in all kind of fields.

This paper provides a qualitative overview of the different fiber sensors based in PCFs. It is structured in five sections. Section 2 explains the geometry-based definition, light guidance and foremost properties in PCFs that make them unique. In Section 3, the applications of PCFs in sensing applications will be detailed. This section is divided in three subsections: physical, chemical, and biosensors. Within Section 4 the technology development opportunities are presented through an overview of the patents of photonic crystal fiber sensors. Conclusions and final remarks are considered in Section 5.

2. Geometry, Guidance Mechanisms, and Properties

Conventional single-mode fibers (SMFs) geometry entails a doped core surrounded by a pure silica cladding (Figure 1(a)), ensuring that the core refractive index is higher than the cladding. Photonic crystal fiber's geometry is characterized by a microstructured air hole cladding running along the entire length of the fiber, which surrounds the core that can be solid or hollow. As so, PCFs can be divided in two families based on their geometry: solid core and hollow-core PCFs. Solid core PCFs, as can be deducted from the name, present a solid core surrounded by a periodic array of microscopic air holes, running along its entire length (Figure 1(b)). Hollow-core photonic crystal fibers (HC-PCFs) present an air hole as core, surrounded by a microstructured air-hole cladding (Figure 1 (c)).

During the modeling as well as the manufacturing process there are different physical parameters to be controlled depending on the kind of fiber to the produced: in an SMF the only parameter to take into account is the diameter of the core, while in a PCF there are three physical parameters to be controlled: the core diameter ρ (which for solid core PCF is defined as the diameter of the ring formed by the innermost air holes), the diameter of the air holes of the cladding-d-and the pitch Λ (distance between the centre of two consecutive air holes). These three physical parameters in combination with the choice of the refractive index of the material and the type of lattice make the fabrication of PCFs very flexible and open up the possibility to manage its properties, leading to a freedom of design not possible with common fibers. Different geometry and different materials will imply different structural design such as to enable different guidance mechanisms through the PCFs: modified total internal reflection (TIR) and/or photonic bandgap guidance (FBG). There are four different guidance mechanisms depending on the PCFs geometry and core/cladding materials [4]:

(i) index-guiding PCF—guides in a solid core through modified TIR;

(ii) PBG-guiding PCF—guides through PBG effect in a hollow-core;

(iii) all-solid PBG PCF—guidance through PBG antiresonant effect in a solid core;

(iv) hybrid PCF—guidance through simultaneous propagation of FBG and modified TIR.

In the following subchapters, single material solid core PCFs and hollow-core PCFs are simply explained, in order to better understand its geometry and the basic guidance mechanisms of PCFs: modified TIR and FBG. For further reading on the guiding mechanisms in different PCFs we encourage the reader to take a look at [4].

2.1. Solid Core PCFs. Solid core PCFs cross-section presents a periodic array of air holes surrounding a solid core, which are extended invariantly along the fiber length. When using a single material in the fiber manufacturing, this cross-sectional configuration leads to a lowering of the cladding's effective refractive index given that the solid core is made of the same material. An illustration of a solid core PCF cross-section structure is presented in Figure 2(a), based in the first PCF presented in 1996 [5], as well as its refractive index

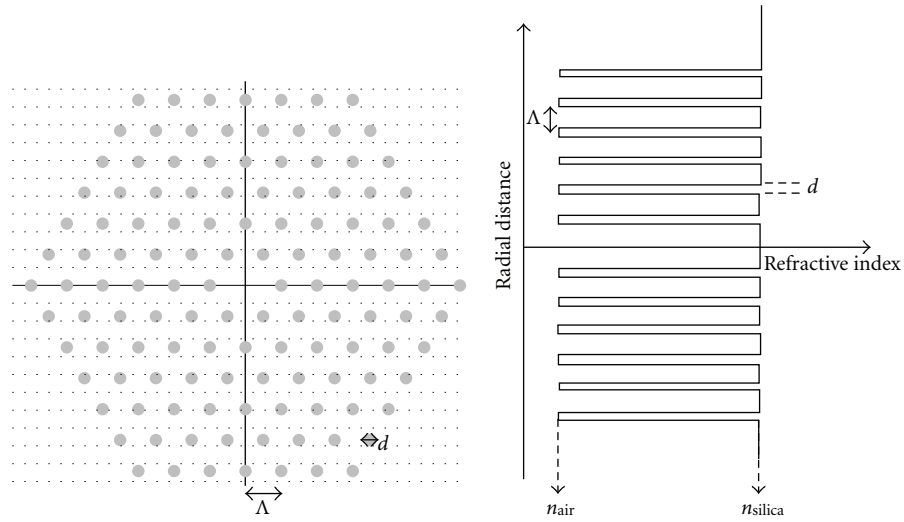

Figure 2: Illustration of (a) solid core PCF cross-section and (b) respective refractive index profile; colors: grey: air, white: silica.

variation with the radial distance in Figure 2(b). In solid core PCFs the refractive index in the cladding will vary with the radial distance, depending on its geometry and material.

The effective cladding refractive index will be lowered when compared with the core's refractive index, allowing the guidance mechanism to be total internal reflection, without the need to dope the core, allowing the solid core PCFs to be made with a single material. Since the light guiding properties of solid core PCFs are not a consequence of spatially varying glass composition, as in standard OFs, but from an arrangement of very tiny and closely spaced air holes, the guidance mechanism is known as modified TIR.

Soli-core PCFs flexibility of design can be explored to achieve endlessly single-mode guidance, even when presenting large-mode areas or high birefringence. These features will lead to outstanding opportunities for applications in ever-widening areas of science and technology, like high power handling [6, 7], fiber laser multiwavelength generation [8, 9], long-period gratings inscribed in the solid core [10], supercontinuum generation [11] applied to optical coherence tomography [12] and to spectroscopy [13], and fiber sensor [14], among others. The last application will be developed in detail in the next section.

2.2. Hollow-Core PCFs. PCFs who present a negative core-cladding refractive index difference cannot operate via TIR (Figure 3). However, an appropriately designed holey photonic crystal cladding, running along the entire length of the fiber, can prevent the escape of light from a hollow core, thus becoming possible to break away from the straitjacket of TIR and trap light in a hollow core surrounded by glass. Under these circumstances, light guiding is only possible if a photonic bandgap exists. Light guidance is then an analogue of a mechanism known in solid state physics as the electron conduction mechanism in materials with an energy-band structure. Periodically distributed air holes can form a 2D photonic crystal structure with lattice constant similar to the wavelength of light. In 2D crystal structures photonic bandgaps exist which prevent propagation of light within a certain range of frequencies. If the periodicity of the structure is broken with a defect, a special region with different optical properties can be created. The defect region can support modes with frequencies falling inside the photonic bandgap, but since around this defect there is a photonic bandgap, light within the defect will remain confined in the vicinity of the defect. Modes falling outside the defect will be refracted, while modes falling inside the defect region will be strongly confined to the defect and guided along it throughout the entire length of the fiber [15].

This effect is illustrated in Figure 4: suppose a hollow-core PCF is designed to work in the red visible region of the electromagnetic spectrum. When the PCF is illuminated by a blue LED, all light will be refracted and no light will be guided by the fiber; consequently no light will come out at the end of the PCF. On the other hand, if the PCF is illuminated by a broadband source the red component of light will be guided appearing at the fiber end and all other frequency components of light (like green or yellow light, represented in Figure 4 for illustrative purposes) will be refracted.

The first bandgap guiding fiber was reported in 1999 [16], demonstrating light confinement and guidance in an air core PCF only at certain wavelength bands, corresponding to the presence of a full 2D band gap in the photonic crystal cladding. This guidance mechanism allows light guidance in air, not possible with standard OFs (for which positive core-cladding refractive index difference is imperative in order to confine light), and presenting noteworthy advantages like extremely small Fresnel reflections, since the refractive index discontinuity between the outside world and the fiber mode can be very tiny; less interaction between guided light and the material forming the fiber core, allowing transmission power levels not possible with conventional fibers, increasing in

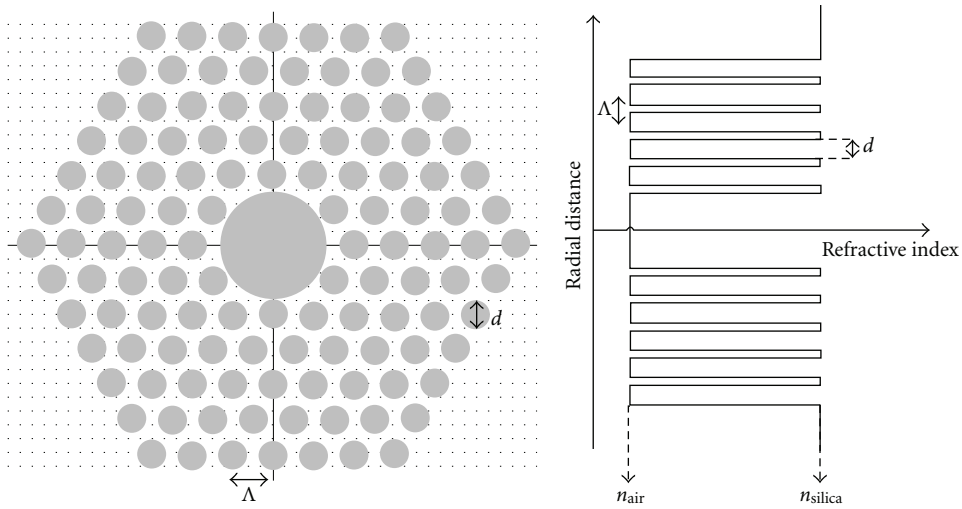

FIGURE 3: Illustration of (a) hollow-core PCF cross-section and (b) respective refractive index profile; colors: grey: air, white: silica.

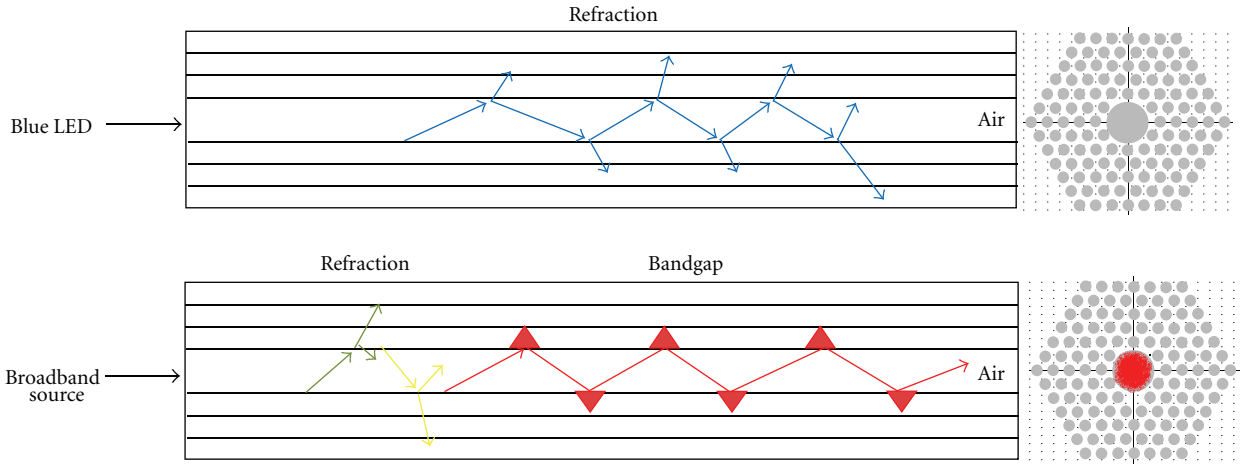

FIGURE 4: Hollow-core PCF guidance of light through PBG.

this way the thresholds powers for lasing based in nonlinear effects; filtering away unwanted wavelengths, since it only works in a range of wavelengths; and the ability to fill the core of the fiber with gases and liquids leading to high light/sample overlapping. These advantages lead to fascinating applications based in HC-PCFs: high power transmission [17], gas-based nonlinear optics [18, 19], optical tweezers propulsion and particle guidance in liquids [20, 21], fiber sensing [22, 23], among others.

3. Sensing Applications

Despite of its youth in the sensing field, PCFs have awakened the interest of many scientific groups due to their promising characteristics. The biggest attraction in PCFs is that by varying the size and location of the cladding holes and/or the core the fiber transmission spectrum, mode shape, nonlinearity, dispersion, air filling fraction and birefringence, among others, can be tuned to reach values that are not achievable with conventional OFs. Additionally, the existence of air holes gives the possibility of light propagation in air, or alternatively provides the ability to insert liquids/gases into the air holes. This enables a well-controlled interaction between light and sample leading to new sensing applications that could not ever be considered with standard OFs. Due to PCFs diversity of features they introduce a large number of new and improved applications in the fiber optic sensing domain [14].

In this section, the applications of PCFs in sensing fields will be detailed, dividing it in two subsections, depending on the parameter that is measured. These two subsections are physical sensors and bio chemical sensors, and each is divided in the several types of sensors.

3.1. Physical Sensors. Physical optic sensors measure physical parameters such as temperature, curvature, displacement,

torsion, pressure, refractive index, electric field, and vibration. The measurement, monitoring, and control of these parameters are of vast interest for several applications. Physical sensors that assess strain/displacement, curvature/bend, transversal load, torsion, and temperature are of immense interest for structural health monitoring. Civil structures like buildings, piles, bridges, pipelines, tunnels, and dams need continuous monitoring with the purpose of controlling and preventing abnormal states or accidents at an early stage, in order to avoid casualties as well as giving maintenance and rehabilitation advice [24]. Physical fiber sensors are perfect for this purpose, since they provide *in situ*, continuous measurement and analysis of key structural and environmental parameters under operating conditions [25, 26]. Other physical sensors like pressure and refractive index find applications in fields such as medicine and bio chemistry, while electric and magnetic field fiber sensors are of enormous benefit for sensing at high voltages, since they provide an insulating link to high-voltage areas (not offered by conventional electric sensors) [27].

3.1.1. Curvature/Bend Sensors. Curvature or bend is an important physical parameter due to its multiarea applications. Application fields such as structural health, robot arms, and artificial limbs insure that lot of attention is paid to the development of these sensors. The first PCF-based bend sensor was presented in 2000 [28]. This bend sensor was developed by the use of a three solid core all-silica PCF used as multiaxis bend sensor, presenting high accuracy in laboratory and in trials on a bridge. A year after, a curvature sensor with a sensitivity of 127 rad/rad was obtained with a two-solid core PCF (made entirely of silica) used as the sensing element, acting as a two-beam interferometer in which the phase difference was a function of the curvature applied to it [29]. Interferometric configurations are in general very popular techniques for the measurement of physical parameters. Sagnac interferometers are very popular for PCF-based fiber optic sensors due to their high extinction ratio, short length of fiber needed (when compared with SMF), and high insensitivity to temperature [30]. Using a highly birefringent (Hi-Bi) solid core pure silica PCF with two asymmetric hole regions in a Sagnac interferometer, curvature measurements were made through the group birefringence, with insensitivity to strain and temperature [31]. In contrast, a curvature fiber sensor was also obtained through a low birefringence solid core silica PCF Sagnac interferometer [32]. Another interferometric configuration often used in the development of fiber sensors is the Mach-Zehnder interferometer (MZI). An all-fiber MZI interferometer for curvature measurement was fabricated by collapsing both ends of an endlessly single-mode (ESM) large-mode area (LMA) pure silica PCF connected to a SMF in a ring down loop [33]. Another ESM silica-core PCF-based MZI was performed by splicing a section of this PCF between two SMFs in order to obtain a bend sensor with a sensitivity of 3.046 nm.m [34]. A temperature insensitive curvature sensor (2.826 nm.cm) was also obtained by producing a core-offset induced interferometer, constructed between a SMF and an all silica solid core polarization maintaining PCF [35]. Long period gratings (LPGs) can also be used as bend sensors. These structures are formed by introducing a periodic perturbation of refractive index or structural geometry along the fiber length, resulting in resonant coupling from the fundamental core mode to copropagating cladding modes which produce a series of attenuation dips in the transmission spectrum. Bending-induced stress to an LPG can be observed by detecting the shift in the resonance wavelength or splitting of the resonance dip. LPGs were inscribed in ESM PCF showing sensitivities of 3.7 nm.m [36] and 27.9 nm.m [37]. A study of bend sensors based in symmetric and asymmetric LPGs inscribed in PCFs was preformed, demonstrating that asymmetric LPGs are spectrally sensitive to bend orientation (showing attenuation bands producing red and blue wavelength shifts) while symmetric LPGs induced bend presented only a unidirectional wavelength shift [38]. Furthermore, a directional bend sensor based in a LPG inscribed in an LMA all-silica PCF was also produced, with a sensitivity of 2.26 nm.m [39].

3.1.2. Displacement/Strain Sensors. There are a number of applications of practical interest in which the monitoring of strain/displacement-induced changes is important. Application areas for which strain/displacement monitoring is important entail experimental mechanics, aeronautics, metallurgy, and health monitoring of complex structures, among others. In order to meet the increasing measurement requirements of modern industry, different types of strain/displacement sensors based on electronic or fiber-optic techniques have been developed. The electrical sensors are the most mature and widely used strain/displacement sensors. The use of the electrical sensor presents several drawbacks such as short lifetime under high temperature, nonlinear distortion, and susceptibility to electromagnetic interference. Compared with the electronic displacement/strain sensors, the fiber-optic-based sensors have the advantages of immunity to electromagnetic interference, light weight, remote sensing ability, and multiplexing capability. The use of PCFs for strain/displacement sensing allows new possibilities and enhanced solutions. To date a number of designs using PCFs have been reported based in polarization and interferometry. A polarimetric strain sensor based in an all-silica Hi-Bi PCF was demonstrated with a sensitivity of 1.3 pm/$\mu\varepsilon$ [40]. Modal interferometers constructed through tapering solid core silica PCFs were also proposed for strain sensing [41, 42]. A high sensitive ($\sim$2.8 pm/$\mu\varepsilon$) wavelength encoded strain sensor was reported to be able to be interrogated by a battery-operated light-emitting diode and a miniature spectrometer, in which the sensing head was a modal interference obtained by splicing a piece of PCF to an SMF [43]. Another modal interferometer was obtained through the structure composed by SMF-PCF-SMF with a core offset at one of the joints. When embedding this interferometer in a cured carbon fiber composite laminate an intensity-modulated microdisplacement sensor presenting 0.0024 dB/μm was obtained [44]. Miniature inline Fabry-Perot (FP) interferometers were also accomplished for strain sensing: by splicing a small length of hollow-core photonic bandgap fiber between two SMFs in order to obtain a strain

sensitivity of 1.55 pm/$\mu\varepsilon$ and insensitivity to temperature and bend [45] or even by multiplexing several FP interferometers based in HC-PBFs between two SMFs to obtain a strain sensor system [46]. Other authors approach to strain sensing was through Hi-Bi PCF-based Sagnac interferometers, as the one presented in Figure 5. Strain sensors developed through Hi-Bi PCF Sagnac interferometers were reported showing temperature insensitivity, using wavelength-based measurement ($\sim$1.11 pm/$\mu\varepsilon$) [47] and intensity-based measurement ($\sim$0.0027 dB/$\mu\varepsilon$) [48]. Using a Hi-Bi PCF in a Sagnac interferometer a displacement sensor was reported with a sensitivity of 0.28286 nm/mm [49]. Through the use of a three-hole suspended-core fiber (SCF) in a Sagnac configuration a displacement sensor was developed with high precision ($\sim$0.45 μm) [50]. An MZI was fabricated by splicing a short length of PCF between two SMFs with collapsed air holes over a short region in the two splicing points. This fiber ringdown loop showed a high strain sensitivity $\sim$0.21 $\mu s^{-1}/m\varepsilon$ and a minimum detectable strain of $\sim$3.6 $\mu\varepsilon$ [51].

3.1.3. Electric and Magnetic Field Sensors. Electric and magnetic field sensing is a very important issue in high- and low-tension structures, such as the ones present in the electric power industry. Conventional sensors usually use antennas, conductive electrodes, or metal connections. Due to their metallic content, conventional sensors are very likely to often perturb the measured parameter. Fiber optic sensors are widely used in these applications because unlike their conventional counterparts, fiber-optic-based sensing techniques minimally disturb the electric or magnetic field, and apart from the sensor head, the connecting fibers are inherently immune to electromagnetic interference. Most importantly, they can provide true dielectric isolation between the sensor and the interrogation system in the presence of very high electromagnetic fields. A wide variety of fiber-optic-based sensing schemes have been proposed and reported to date. However, such schemes have a number of disadvantages such as high coupling losses, limited mechanical reliability, and difficulties in mass production. Ideal fiber-based field sensors should present properties such as small size, simple design, and an all-fiber configuration with high measurement accuracy. A polarimetric sensing scheme with selectively liquid-core-(LC-) infiltrated Hi-Bi PCF (infiltrated section <1 mm) was demonstrated for electric field sensing with a sensitivity of $\sim$2 dB per kV_{rms}/mm [52]. LCs are materials which present external field-dependent optical anisotropy and high birefringence. Infiltration of LC materials makes the PCF susceptible to external field variations, a property which can be utilized to fabricate all-fiber current sensors [53, 54]. The directional electric field sensitivity of the same LC-infiltrated PCF probe was also demonstrated, showing that the sensor probe has higher sensitivity to the electric field component aligned along the Hi-Bi PCF axis [55]. An intensity-measurement-based electric field sensor was reported by infiltrating an LMA PCF with an LC (infiltrated section <1 cm), demonstrating a sensitivity of $\sim$10.1 dB per kV_{rms}/mm in transmission and $\sim$4.55 dB per kV_{rms}/mm in reflection [56]. The growth of magnetic field PCF-based sensors is at slow pace. The development of a spun elliptically birefringent PCF with reduced temperature dependence [57] showed the advantages of this PCF over conventional spun stress birefringence fibers, opening the possibility for magnetic sensing with PCFs. The development of a magneto-optic Faraday effect in a miniature coil wound from a six-hole spun PCF [58] provided information about the ability of this PCF to efficiently accumulate Faraday phase shift in a magnetic field even when the fiber is wound into a coil of very small diameter. By using a Hi-Bi PCF injected with a small amount of Fe_3O_4 nanofluid a sensitivity of 242 pm/mT was shown [59]. A magnetic field sensor based on the integration of a high birefringence photonic crystal fiber and a composite material made of Terfenol particles and an epoxy resin was demonstrated with a sensitivity of 0.006 nm/mT over a range from 0 to 300 mT with a resolution $\pm$1 mT [60]. Recently, a magnetic field measurement sensitivity of $\sim$33 pm/Oe was obtained using an HC-PCF sensor based on the characteristic of magnetic-controlling refractive index [61].

3.1.4. Pressures Sensors. Pressure measurements are required in various industrial applications within extremely harsh environments such as turbine engines, compressors, oil and gas exploitations, power plants and material processing systems. Conventional sensors are often difficult to apply due to the high temperatures, highly corrosive agents or electromagnetic interference that may be present in those harsh environments. Fiber optic pressure sensors have been proved themselves successful in such harsh environments due to their high sensitivity, wide bandwidth, high operation temperature, immunity to electromagnetic interference, lightweight and long life. Using periodically tapered LPGs written in a ESM PCF, measurements of hydrostatic pressure up to 180 bar showing a pressure sensitivity of 11.2 $pmbar^{-1}$ were carried out [62]. A very popular technique for pressure sensing is polarimetric measurement. Several authors reported polarimetric studies and measurements leading to the development and application of pressure sensors based in the commercial Hi-Bi PCF: a study of pressure sensing with this PCF at three different temperatures showed its temperature insensitivity, while simultaneously measuring pressure variations [63]; an intensity measurement of pressure with a sensitivity of 2.34×10^{-6} MPa^{-1} was later demonstrated [64]; and a wavelength measurement of pressure variation was shown to provide a sensitivity of 3.38 nm/MPa with an operating limit of 92 MPa [65], which lead to an practical application, Tsunami sensing, since the high pressure sensitivity join with temperature insensitivity makes this sensor suitable to work in a harsh environment such as the ocean bottom [66]. Other polarimetric sensors were developed based in home-made Hi-Bi PCFs: a polarimetric measurement to a specially designed fiber showed a pressure of -10 rad/(MPa·m) [67]; by using two fibers with a small number of cladding holes with different diameters, in order to induce birefringence, a sensitivity up to 23 rad/MPa·m was obtained [68]; and using two different germanium doped-core Hi-Bi PCFs to measure pressure a sensitivity that exceeds 43 rad/MPa·m and low sensitivity to temperature were reported [69]. As for so many other

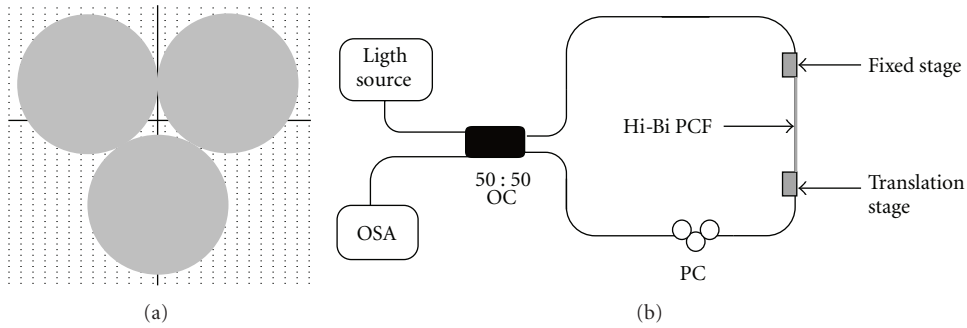

Figure 5: Schematic representation of (a) three-hole SCF cross-section [grey-air, white-silica] and (b) Sagnac interferometer set up for strain measurement.

physical sensors, the Sagnac interferometer configuration is also used to sense pressure. Using a commercial Hi-Bi PCF in a Sagnac interferometer a temperature insensitive pressure sensor with 3.42 nm/MPa at 1550 nm was obtained [70]. This sensor sensitivity was later improved by the utilization of the Hi-Bi PCF coiled inside the Sagnac loop, reaching a sensitivity of 4.21 and 3.24 nm/MPa at 1320 nm and 1550 nm, respectively [71]. Through the use of a four-hole SCF, two different interferometric configurations were used for pressure sensing, showing two very different sensitivities to pressure with residual temperature sensitivity [72]. One of the configurations is a FP cavity made by splicing the SCF in between a SMF and a hollow-core fiber, showing sensitivity to pressure variations of 4.68×10^{-5} nm/psi. And the other configuration, showing much higher sensitivity (0.032 nm/psi), is made through a Sagnac interferometer with the SCF.

3.1.5. Temperature Sensors. Fiber optic sensors have proven to be very useful in measuring temperatures in basic metals and glass productions, in critical turbine areas typical in power generation operations, rolling lines in steel, furnaces of all sorts, sintering operations, ovens and automated welding equipment (which often generate large electrical fields, disturbing conventional sensors). Other applications were OFs-based temperature measurement is quite efficient is in high temperature processing operations in cement and chemical industries. Semiconductor industry also takes advantage of FO remarkable characteristics in temperature sensing, especially in fusion, sputtering, and crystal growth processes. Industries such as civil, aerospace, and defense make lot of use of this sensor to monitor and control their structures health. This kind of FO sensor is one of the most required in the commercial market due to the high number of applications in so different areas. Consequently, temperature-based PCFs sensors were quickly developed aiming to produce new sensors with improved characteristics, mainly improved sensibility and stability. Studies to understand the influence of the geometry and the material quality in the Hi-Bi PCF sensitivity to temperature were developed [73]. A polarimetric interrogation to this kind of Hi-Bi PCF showed a sensitivity of 0.136 rad/°C at 1310 nm [74]. Using modal interference other temperature sensors were reported: by tapering a solid silica-core PCF, a sensitivity of 12 pm/°C was obtained for measurements up to 1000°C [75]; using an LMA PCF spliced to an SMF a three-beam path modal interferometer with a sensitivity of 8.17 pm/°C was reported [76]; a strain-independent modal interferometer for temperature sensing (sensitivity ~73 pm/[a]C) was accomplished by an induced core offset of a nonlinear PCF in-between of a multimode fiber (MMF) and a SMF [77]. MZIs using LPGs in a PCF with a sensitivity of 42.4 pm/°C [78] and an all-solid PBF (doped fiber) with enhanced temperature sensitivity 71.5 pm/°C were demonstrated [79]. Hybrid FP structures were also developed for temperature sensing: been by forming a sensing head by two FP cavities formed by fusion splicing a PCF with a short peace of hollow-core fiber and an SMF in series [80], or by splicing SMF to a short piece of SCF (end cleaved) forming a miniature FP sensor head and interrogating it with a dual-wavelength Raman fiber laser for unambiguous temperature recovery (sensitivity ~0.84 deg/°C) [81], or by inserting the FP interferometer in a laser cavity as a mirror for simultaneous sensing and lasing (sensitivity ~6 pm/°C) [82]. The inscription of LPGs in a solid core PCF was also tried for temperature sensing showing a sensitivity of 10.9 pm/°C [83]. Sagnac interferometers were built making use of filled PCFs for temperature sensing: using a two-hole birefringent PCF filled with metal indium it was possible to achieve a sensitivity of 6.3 nm/K [84] and by filling a Hi-Bi PCF with alcohol a sensitivity as high as 6.6 nm/°C was reached [85]. Sagnac interferometers do not only use filled PCFs for temperature sensing. In reality, the most common and recent approach for temperature measurement using PCF is filling them with a liquid. By filling the fiber with quantum dots two different temperature sensors were developed: been by depositing quantum dots nanocoatings through the Layer-by-Layer technique in the inner holes of an all-silica LMA ESM PCF with a resultant sensitivity of 0.1636 nm/°C [86] or by inserting them in a hollow core of a PCF obtaining a sensitivity of 70 pm/°C [87]. By filling the air holes of the cladding of a solid core PCF with Fe_3O_4 nanoparticle fluid a temperature sensitivity of 0.045–0.06 dB/°C depending on the length of the fiber (5 cm–10 cm) was accomplished [88]. By filling 10 cm of solid core PCFs with a less expensive liquid like ethanol a sensitivity of

0.315 dB/°C was reported [89]. When selectively infiltrating one of the air holes of a solid core PCF with a 1.46 refractive index liquid the sensitivity to temperature was proved to be ∼54.3 nm/°C [90]. Distributed Brillouin temperature sensing was also accomplished using PCFs: through the use of a germanium doped-core birefringent PCF with variations of 0.96–1.25 MHz/°C [91] and by using the birefringent effect of a transient Brillouin grating in a polarization-maintaining PCF leading to a sensitivity of 23.5 MHz/°C [92].

3.1.6. Torsion/Twist Sensors. Torsion measurement and control is important in civil engineering applications such as bridges, buildings, and others. A polarimetric torsion sensor based in a Hi-Bi PCF (see Figure 6) was reported to present a sensitivity of ∼0.014/° in a linear twist angle ranging from 30° to 70° [93]. Several Sagnac-based structures were reported for torsion sensing: a two-LP-mode operation Hi-Bi PCF was demonstrated to measure the twist angle with a resolution of ∼2.7° and low sensitivity to temperature [94]; a temperature and bend insensitive torsion sensor based in Hi-Bi PCF with enlarged air holes in one axis was achieved, showing a sensitivity of ∼0.06 nm/° [95]; a sensor able to measure the torsion angles and direction simultaneously was reported though a side-leakage PCF (sensitivity ∼0.9354 nm/°) [96] and a Sagnac based in an LMA PCF torsion sensor was reported with a sensitivity of 1 nm/° and a resolution of 0.01° [97]. The use of LPGs is also common for this kind of sensor: by mechanically inducing an LPG in an all-silica solid core PCF a torsion sensitivity of 0.73 nm/2π was obtained [98] and by inducing LPGs in two different PCFs a dependency on the asymmetry of the cladding structure is noticed to obtain high sensitivity 12.4 nm/(rad/cm) [99].

3.1.7. Transversal Loading Sensors. Transversal load is also a very important parameter to monitor and health of civil structures. A polarimetric transverse load sensor was reported using a Hi-Bi PCF with larger air holes on one axis, presenting a sensitivity of ∼2.17 nm/(N/cm) [100]. Several authors opted for inscribing fiber Bragg gratings (FBGs) in solid core PCFs. By using an FBG in a two-hole PCF, a sensitivity of 17.6–26 pm/(N/cm) was shown [101]. By embedding an FBG Hi-Bi PCF in a reinforced composite material a sensitivity of 15.3 pm/MPa was achieved [102]. This leads to a study of transversal load characteristics in different PCFs with inscribed FBGs. This study reported that increasing transverse load shifts the Bragg wavelength to longer values and that the FBG PCF sensitivity to transverse load decreased with increasing volume of air-holes around the core, and even more, a dependence on the fiber orientation was observed [103]. A four-hole SCF was inscribed with FBGs and tested for transverse load. It was demonstrated that SCFs experience sensitivities going from 2.19 pm/(N/cm) to 12.23 pm/(N/cm) depending on where the load is applied transversely [104]. Other structures also used in transversal load sensing are Sagnac interferometers. Two Sagnac interferometers were developed based in the same LMA PCF for transverse load measurement: by measuring the transverse displacement of the PCF coil (sensitivity of 90.4 nm/mm), the sensitivity to load variations is enhanced while the sensitivity to temperature is decreased, when compared with the SMF case [105]; and by direct measurement of the transmission spectrum shift corresponding to the measured mechanical load a sensitivity of 0.519 nmN^{-1} mm^{-1} was achieved [106].

3.1.8. Refractive Index Sensors. Refractive index is a fundamental material property. Consequently, its accurate measuring is crucial in many applications. In food or beverage industries, the monitoring of refractive index is part of the quality control, and the development of simple and compact refractometers is key. Optical fiber refractive index sensors are attractive, owing to their small size, flexibility in their design, immunity to electromagnetic interference, network compatibility, and the aptitude for remote and *in situ* measurements. FBGs writing in a three-hole germanium-doped-core SCF were reported with a resolution of 3×10^{-5} and 6×10^{-6} around mean refractive index values of 1.33 and 1.4 [107]. LPG-based devices offer high sensitivity to the refractive index variations of the surrounding medium. Refractive index measurement within a solid core PCF inscribed with LPGs was reported, where the coherent scattering at the cladding lattice is used to optically characterize materials inserted into the fiber holes—liquid water to solid ice transition is characterized through the refractive index determination [108]. A high sensitive refractive index sensor based in LPGs inscribed in an ESM PCF was reported presenting a wavelength-measured sensitivity of 440 nm/RIU and an intensity-measured sensitivity of 2.2 pm/°C [109], presenting suitable characteristics for applications such as label-free bio sensing [110]. By inscribing LPGs in air and water filled solid core PCFs an excellent sensitivity of $\sim 10^{-7}$ RIU within a index range of 1.33 and 1.35 for air-filled was shown [111]. A highly sensitive approach (1500 nm/RIU) was reported based in LPGs inscribed in a LMA PCF (see Figure 7(a)) [112]. Modal interference seems to be a very used technique for refractive index sensing with PCFs. A LMA tapered PCF with collapsed air holes was demonstrated for refractive index sensing with a resolution of 1×10^{-5} RIU [113] and direct application in gas sensing [114]. The core mode couples to multiple modes of the solid taper waist, which can be seen at the output as interference peaks that shift with refractive index variations. Another approach taken was an in-reflection PCF interferometer (see Figure 7(b)), obtained by splicing an SMF to an LMA PCF [115]. In the splice, the voids of the PCF are collapsed allowing coupling of PCF core and cladding modes. An ultrasensitive PCF-based refractive index was reported with a sensitivity of 30100 nm/RIU, by inserting the fluid in one of the adjacent air holes to the core [116]. The core mode can couple with the mode of this microfluidic channel with a strong field overlap. Another two modal interferometer-based refractive index PCF sensors were developed: one based in an LMA spliced between two SMFs presenting a maximum resolution of $\sim 2.9 \times 10^{-4}$ RIU [117] and the other based in two large-core air-clad PCF spliced in between SMFs in series, presenting a resolution

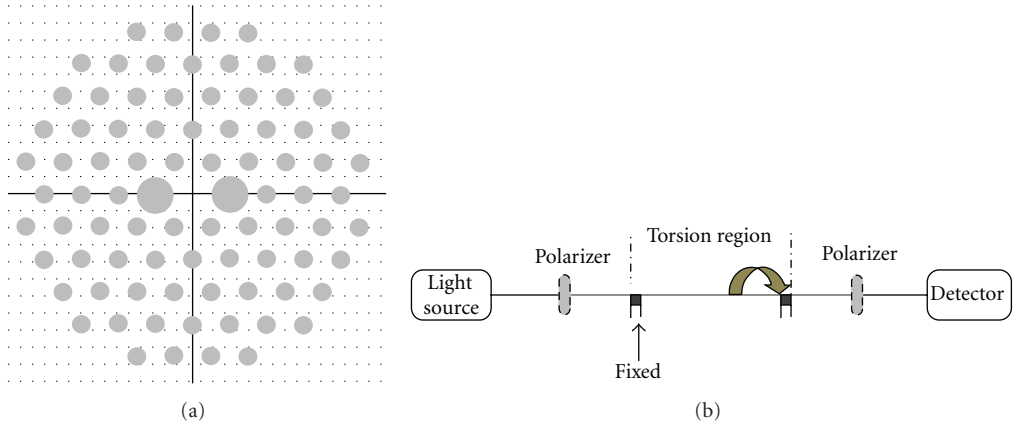

Figure 6: Schematic representation of (a) Hi-Bi PCF cross-section (grey: air, white: silica) and (b) polarimetric configuration for torsion measurement.

of $\sim 3.4 \times 10^{-5}$ RIU [118]. The refractive index response of a modal interferometer based on a PCF using a thin plasma deposited silicon nitride overlay with high refractive index was demonstrated, showing improved refractive index sensitivity [119]. An MZI-based refractometer was also developed using a LMA PCF in a cavity ringdown loop, with a resolution of 7.8×10^{-5} RIU [120]. A refractive index sensor based in four-wave mixing (FWM) in a PCF was reported presenting a high sensitivity of $\sim 8.8 \times 10^{3}$ nm/RIU [121]. Photonic bandgap-based refractive index sensing was as well demonstrated: by a wavelength shift falling inside the PBG due to refractive index variations (resolution of 2×10^{-6} RIU) [122], or by observing the PBG shift in two types of all-solid core PCF with a series of high refractive index infiltrations (resolution of $\sim 10^{-6}$ RIU) [123], or even by using a hollow-core low-refractive index contrast Bragg fiber to infiltrate different aqueous analytes in order to observe high refractive index sensing (sensitivity ~1400 nm/RIU) [92].

3.1.9. Vibration Sensors. The dynamic loading of a structure gives rise to induced vibrations, which usually occur at a frequency close to the natural frequency of such structure, potentiating structural or mechanical failure, which results in severe damage to the structure in certain situations. In this context, monitoring and detecting damage caused by vibrations in structures at an early stage is very important. As so controlling constantly, and possibly remotely, parameters such as the vibration amplitude and frequency are extremely important to detect structural damages in rotor blades, aircraft fuselages, and wing structures, and so forth. Fiber optic sensors play a special role in this field due to their small size, immunity to electromagnetic interferences, and, in the case of using single material PCFs, high insensitivity to temperature variations. Only recently, vibration measurements using PCFs were demonstrated: by using a Hi-Bi PCF embedded in a glass-fiber-reinforced polymer for high sensitivity vibration measurements up to 50 Hz [124] and by using a polarization maintaining PCF embedded also in a glass polymer composite material showing reliable frequency and amplitude measurements of vibrations and with a sensitivity of ~0.253 dB/mm [125]. In both fiber sensors, polarization maintaining or Hi-Bi PCFs were chosen due to their negligible level to temperature-vibration cross coupling.

3.1.10. Multiparameter Sensing. Several sensors are able to measure two or more parameters simultaneously. The most common parameters simultaneously measured are strain and temperature. A distributed Brillouin sensing system was developed through the use of a germanium-doped PCF, resulting in a highly precise simultaneous measurement of temperature (sensitivity ~0.96–1.25 MHz/°C) and strain (sensitivity ~0.048–0.055 MHz/$\mu\varepsilon$) [126]. By amplifying a Hi-Bi PCF through an erbium-doped fiber, a polarimetric measurement of temperature and strain was made presenting sensitivities of 0.04 dB/°C and 1.3 pm/$\mu\varepsilon$, respectively [127]. An FBG inscribed in a erbium-doped-core PCF showed a sensitivity to strain of 1.2 pm/$\mu\varepsilon$ and a sensitivity to temperature of 20.14 pm/K [128]. Strain and temperature simultaneous measurement was also demonstrated using FP cavities. A hybrid FP cavity was obtained by splicing SCF at the end of an SMF, using three-hole and four-hole SCFs. The hybrid structure characterization was done through wavelength and phase variations: the strain sensitivity was 1.32 pm/$\mu\varepsilon$ and 10.4 rad/m·$\mu\varepsilon$ for the three-hole SCF case and for the four-hole SCF 1.16 pm/$\mu\varepsilon$ and 8.5 rad/m·$\mu\varepsilon$; the temperature sensitivity for the three-hole SCF was 7.65 pm/°C and 67.8 rad/m·°C and for the four-hole SCF 8.89 pm/°C and 67.6 rad/m·°C [129]. Other FP configuration was developed by splicing an HC-PCF in-between two SMFs, presenting sensitivities to temperature and strain of 1.4 pm/°C and 5.9 nm/$\mu\varepsilon$, respectively [130]. As it is for individual strain and temperature measurements, for the simultaneous measurement of these two parameters the Sagnac interferometer is a very popular approach. A Sagnac interferometer was developed based in a four-hole SCF, resulting in a strain sensitivity of ~1.94 pm/$\mu\varepsilon$ and temperature sensitivity of ~0.3 pm/°C [131]. By using a Hi-Bi PCF in a Sagnac configuration previously amplified by an erbium-doped fiber, strain and temperature can be

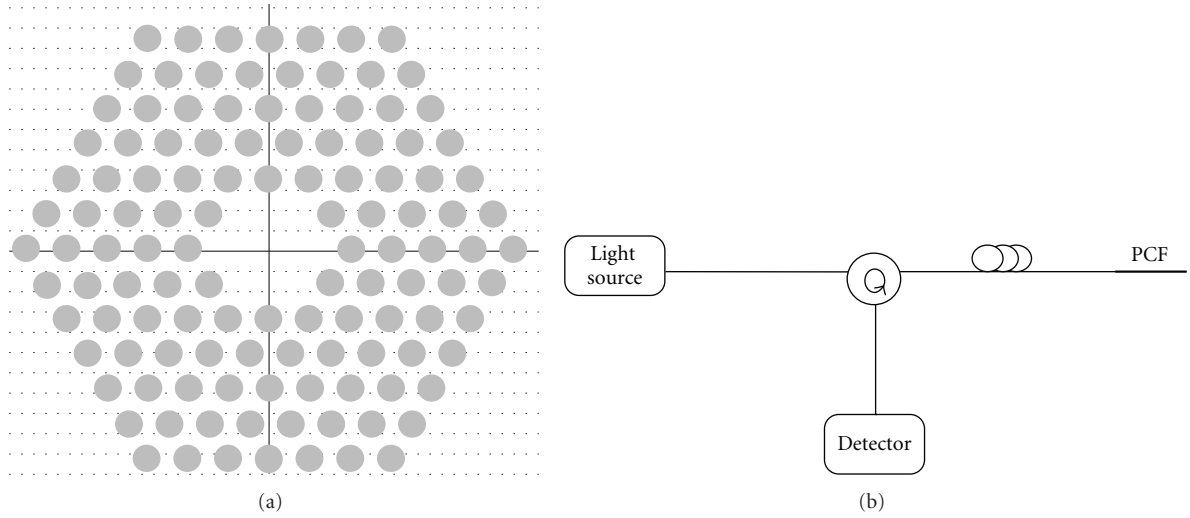

Figure 7: Schematic representation of (a) LMA PCF cross-section (grey: air, white: silica) and (b) in-reflection set up for refractive index measurement.

separately discriminated presenting a sensitivity of 1.3 pm/$\mu\varepsilon$ and 0.3 pm/°C [132]. With a small-core Hi-Bi PCF-based Sagnac loop, strain and temperature can be measured with resolutions of $\pm 4.7\,\mu\varepsilon$ and ±1.5°C, respectively [133]. A Sagnac loop using an elliptical hollow-core PBF was reported with a sensitivity of 0.81 pm/$\mu\varepsilon$ to strain and of 3.97 pm/°C to temperature [134]. Configurations using two concatenated Sagnac interferometers were also used for temperature and strain sensing: by using a Hi-Bi PCF in one and an elliptical cladding fiber on the other Sagnac loop resolutions of $\pm 21\,\mu\varepsilon$ and ±1.1°C were achieved [135]; using a reference and a sensing interferometer (with a all-solid hybrid PCF) a strain sensitivity of 25.6 pm/$\mu\varepsilon$ and a temperature sensitivity of 9 pm/°C, with suppressed crosstalk 0.33 $\mu\varepsilon$/°C, were achieved [136]. Modal interferometry was also used for temperature and strain simultaneous measurement: by connecting a piece of HC-PCF in both ends to SMFs, an interferometer with resolutions of $\pm 1.4\,\mu\varepsilon$ and ±0.2°C was achieved for strain and temperature, respectively [137]; another modal interferometer was constructed by making two tapers in a boron-doped Hi-Bi PCF, reaching sensitivities of 2.51 nm/$\mu\varepsilon$ for strain and 16.7 pm/°C for temperature [138]; a modal interference-based array of sensors, using short lengths of solid core PCF spliced between SMFs, was reported showing the individual sensors sensitivities to strain and temperature of 2.2 pm/$\mu\varepsilon$ and 7–9 pm/°C [139]. Simultaneous measurements of curvature and strain were also reported: by using a suspended multicore fiber [140] or by forming an MZI in a solid core LMA PCF with sensitivities of 3 pm/$\mu\varepsilon$ to strain and 36 nm/m to bending [141]. A fiber sensor was reported that could measure simultaneously pressure and strain based in a Hi-Bi PCF showing a polarimetric sensitivity of 14.8 rad/MPa·m to pressure and 2.8 rad/m·$\mu\varepsilon$ to strain [142]. Pressure and temperature are parameters that were also reported to be measured simultaneously using a twin-core fiber: by inscribing FBGs in the fiber, a linear relationship between pressure and peak shift is obtained for 2000 psi and a sensitivity to temperature of 14.9 pm/°C [143]; using thermally regenerated FBGs in the fiber sensitivities to pressure and temperature of 13.3 pm/psi and 15.18 pm/°C were obtained, respectively [144]. Simultaneous measurement of load and temperature was accomplished though writing LPGs in the joint of a PCF with an SMF achieving sensitivities of 2.18 nm/N and 0.086 nm/°C, respectively [145]. An inline FP tip sensor was developed by splicing an ESM PCF between two SMFs for refractive index and temperature sensing, presenting sensitivities of 4.59/RIU and 4.16 nm/°C, respectively [146]. Measurements of three parameters simultaneously have been reported. By using a solid core PCF in a specially developed spectral interferometric method temperature, strain and pressure were measured with precisions of $1.28 \times 10^{-5}\,\mathrm{K}^{-1}$, $0.4\,\varepsilon^{-1}$ and 10^{-5} MPa, respectively [147]. A arc-induced LPG in a PCF showed sensitivity to temperature (~6 pm/°C), strain (2.5 pm/$\mu\varepsilon$) and bending (12.4 nm/m) [148]. Using a Sagnac interferometer with a section of polarization maintaining side-hole fiber torsion, strain and temperature were measured with sensitivities of 0.06–0.08 nm/°, 0.016–0.21 nm/$\mu\varepsilon$, and 1.44–1.97 nm/°C, respectively [149]. Using a suspended twin-core fiber an all-fiber MZI is obtained which is able to measure curvature (1.35–1.42 nm·m), temperature (18.2–34.9 pm/°C), and strain (5-5.6 pm/$\mu\varepsilon$) [150].

3.2. Bio Chemical Sensors. Optical fibers can be used for sensing of chemical and biological samples. OF-based sensors are advantageous for chemical and bio sensing due to their miniaturization, small size, flexibility, and remote capability, making fibers suitable for *in vivo* experiments, due to the fact that these waveguides are electrically passive, not representing a risk to patients, since there are no electrical connections to their body, and due to the ability for real-time measurement and the possibility to simultaneously measure several parameters. One approach for chemical/bio sensing is to provide the fiber end with a suitable indicator or a material that

responds to the parameter of interest. Chemically sensitive thin films deposited on selected areas of optical fibers can influence the propagation of light in such fibers depending on the presence or absence of chemical/biological molecules in the surrounding environment. A wide range of optical sensors has been developed for selective biomolecule detection. Most of them have reliability issues as they employ very fragile antibodies as sensing elements [151].

When compared to the conventional OFs, PCFs offer a number of unique advantages in chemical and bio sensing applications. Due to the presence of air holes running along its entire length, these fibers have a unique ability to accommodate biological and chemical samples in gaseous or liquid forms in the immediate vicinity of the fiber core or even inside the core. PCFs can be used simultaneously for light guiding and as a fluidic channel, leading to a strong light/sample overlap. Such channels can be further functionalized with biorecognition layers that can bind and progressively accumulate target biomolecules, thus enhancing sensor sensitivity and specificity. Due to PCFs core and cladding air holes small size and the high overlapping between sample and light, a very small fluid volume is required for sensing. Using PCFs the amount of volume needed is of the order of hundreds of nanoliters to tens of microliters, while in conventional optics measurement techniques the volumes needed are of order of one to ten milliliters. The use of extremely small volume is of huge interest for chemical and biomedical applications, like analytes detection or protein/DNA recognition [152, 153].

3.2.1. Gas Sensors. Many industries produce gaseous emissions as a consequence of the processes they develop. Chemical processing, glass melting, metal casting, transportation, pulp and paper, and energy production industries all produce different amount and types of gaseous emissions. As so, monitoring and control gas has become an increasingly important consideration in an ever-broader global environmental awareness context. For other industries such as chemical, bio chemical, and military ones, gas diffusion is as important parameter to analyze. Therefore, it is of enormous importance to develop gas sensing techniques that are selective, quantitative, fast acting, and not susceptible to external poisoning. To satisfy these requirements PCFs are employed, the air holes running the entire length of the fiber will act as microsized capillaries allowing gas diffusion to take place, and the whole process can be monitored, see Figure 8. PCFs are very attractive for fast, real-time detection and measurement of simple gases. Even more, PCFs technology is compatible with telecommunications systems and can easily exploit remote sensing and multiplexing.

(1) Acetylene Sensors. Different methods were reported to measure acetylene. When using solid core PCFs the most common technique is evanescent wave absorption. Some gas molecules exhibit characteristic vibrational absorption lines in the near-IR region corresponding to the transmission window of silica-based fibers and as so can be detected through the evanescent field of the guided mode. The presence of such molecules is visible in the air holes of the fiber since a loss appears in the transmission spectrum for the characteristic wavelengths of the particular gas species. The first approach to this technique was through the use of a solid core hexagonal lattice PCF [154] and two years later through a solid core random-hole PCF using *in situ* bubble formation technique [155]; positive results were also reported using a three-hole SCF [156]; more recently, using a solid core PCF with FBGs inscribed in it presenting a sensibility of ~0.017–0.022 dB/% to acetylene concentration [157]. Acetylene sensing was also developed using HC-PCFs. Gas diffusion inside of an HC-PCF was successfully monitored by measuring the attenuation of the guided light through the fiber due to absorption of light by the gas sample [158]. Another approach made using saturation absorption spectroscopy inside of a large core HC-PCF (20 μm core) reported narrower transition and cleaner signals than when using smaller-core HC-PCFs [159]. A cell, made through filling an HC-PCF with gas and then splicing it to SMFs, containing an acetylene volume <5 μL, was used to measure its concentration through correlation absorption spectroscopy [160]. This configuration advantage is the reduced hazard even when filled with explosive or harmful gases.

(2) Methane Sensors. Detecting methane is of special relevance in many industrial and safety applications. For gas detection, spectral sensors preferably address the strongest absorption lines. For methane, these are found in the midinfrared spectrum around 3300 nm. Despite the fact that in this wavelength region light sources and detectors are expensive methane sensing has been reported around these wavelengths [161]. Most of the authors, due to these economic inconveniences, try to work in less challenging wavelength regions. A methane sensor working at 1670 nm was developed through absorption spectroscopy for gas concentration inside of a HC-PCF, with a minimum of detection of 10 ppmv [162]. Using an HC-PCF as a gas cell for methane sensing at 1300 nm, a sensitivity of 49 ppmv-m was reported [163]. Methane sensing was also accomplished using an HC-PCF as a gas cell, targeting two different wavelength bands in the near-infrared region [164]. And, a fast response methane sensor with periodic side openings microchannels in a HC-PCF was demonstrated with a sensitivity of ~647 ppm [165].

(3) Multigases Sensors. Several other gases sensors have been developed, almost all based in evanescent field absorption spectroscopy. A hydrogen sensor was reported based in a tapered soli-core PCF with collapsed air holes coated with thin layers. The collapse holes allow access to the evanescent field that could be absorbed with gas-permeable thin films [166]. The detection of volatile organic compounds was demonstrated through an in-reflection PCF interferometer, without the need of any permeable material [167]. Through the measurement of gas diffusion coefficient acetylene and air were detected in a solid core PCF [168]. An all-fiber gas sensing system was developed based in an HC-PCF as a gas cell, achieving minimum concentration detectable values of 300 ppm for carbon dioxide and 5 ppm for acetylene [169]. Characterization of the absorption lines of acetylene,

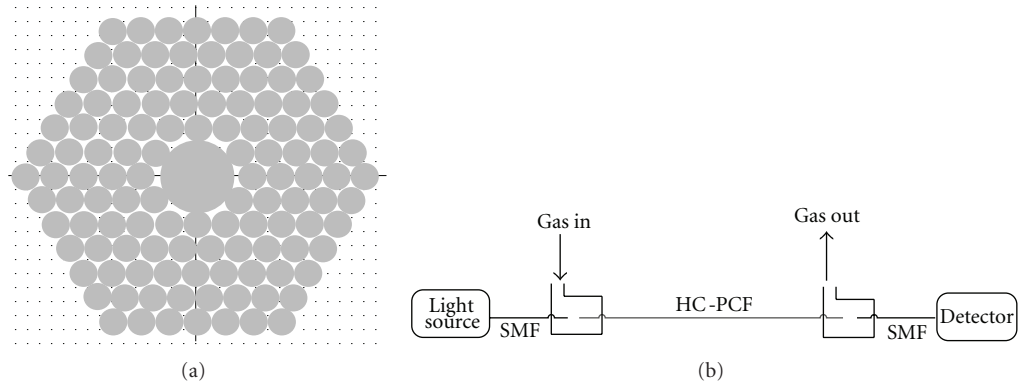

Figure 8: Schematic representation of (a) HC-PCF cross-section (grey: air, white: silica) and (b) configuration for gas sensing using PCFs.

hydrogen cyanide, methane, and ammonia was shown to be possible using a PBF spliced to an SMF in one end and filled with gas through the other [170]. Saturated absorption in overtone transitions of acetylene and hydrogen cyanide molecules confined in an HC-PBG was observed using input powers as low as 10 mW [171]. In another approach, spontaneous gas-phase Raman scattering using a HC-PBF as a gas cell was reported to successfully detect methane, ethane, and propane Raman signatures [172]. Even more, oxygen and nitrogen detection was performed using spontaneous Raman backscattering [173]. The implementation of a PBF-based gas sensor designed and built for practical use, occupying a small volume within preexisting equipment, was demonstrated for the detection of methane and acetylene gas [174]. Recently, an inline sensor based in two pieces of an HC-PBF with laser-drilled lateral micro-channels for gas access was reported [175], showing the ability to quantitatively measure gas mixtures. An oxygen gas sensor was also reported by forming fluorophore-doped sensing film in the array microholes of a solid core PCF, with a sensitivity of 10.8 (defined as I_0/I_{100}) and quick response time ~50 ms [176].

3.2.2. Molecular Sensors. A molecular sensor is based in a molecule that interacts with an analyte to produce a detectable change. Molecular sensors combine molecular recognition with some form of reporter so the presence of the guest can be observed. This kind of sensors is very important for applications such as biochemistry or biomedicine for which the detection of molecules like DNA, proteins and cancer cells are of huge importance, as it is the use of the lower sample volume possible. PCFs microstructured channels make these fibers very appropriate for such applications, given that they can be used to control the interaction be-tween guided light and fluids located within the holes while simultaneously acting as a tiny sample chamber. Two big advantages can be obtained with these fibers: high overlapping between light and sample which is not possible with OFs or typical spectroscopy measurement techniques and the ability to perform the measurement with a very little volume sample, typically μL or less, that is much lower than in conventional spectroscopy (mL).

Rhodamine Sensors. Rhodamine belongs to the family of fluorone dyes that are often used as a tracer dye. Rhodamine dyes are used extensively in biotechnology applications such as fluorescence microscopy, flow cytometry and for the detection of analytes. This compound has well-known characteristics, and as so is one of the most used for proof-of-concept experiments, especially in molecular and fluorescence experiments. Mainly two types of techniques are used to proof detection efficiency of rhodamine: fluorescence based techniques and surface-enhanced Raman scattering. Fluorescent measurements are an invaluable tool in the study of biological systems and processes. The two most important and widely used applications of fluorescence in biomedical research are fluorescence microscopy and flow cytometry. FCFs can be used in this context for delivery of the excitation light, allowing *in vivo* fluorescence measurements by exciting the desired region, and for detection of fluorescence. A double-clad PCF was used to excite and detect the fluorescence of a rhodamine 6 G dye gelatin sample, showing enhanced detection efficiency [177]. A highly sensitive gold-coated side-polished D-shaped PCF was subjected to the excitation of surface plasmon resonance technology. The plasmonic fluorescence emission of Rhodamine B using a PCF was found to be enhanced [178]. There has been significant interest in using SERS and fibers for chemical, biological, and environmental detections. The combination of both offers the advantages of the molecular specificity of Raman scattering, the big enhancement factor of SERS, and flexibility of fibers [179]. Rhodamine B detection through a four-hole SCF with gold nanoparticles serving as substrate was presented, with large interaction volume between the excitation light and the nanoparticles [180]. By filling hollow-core PCFs with aqueous solutions and using SERS, the following molecules, in a solution with the silver nanoparticles, were identified: rhodamine 6 G [181]; rhodamine 6 G, human insulin and tryptophan with sensitivity of 10^{-4}–10^{-5} M [182]; rhodamine 6 G with the lowest detectable concentration (10^{-10} M) [183]. A study with different PCFs (one solid core PCF and two three hole SCF) for molecular detection using SERS was reported, in which the SCF was found to be the more adequate for the purpose demonstrating a sensitivity of 10^{-10} M to

rhodamine 6 G in an aqueous solution of only ~7.3 μL of volume [184].

DNA Sensors. DNA analysis techniques are usually performed by immobilizing a single strand of DNA on a glass chip and checking the hybridization of this strand to its complementary. The glass surface needs a functionalization treatment in order that the binding of biological species takes place, and hybridization is later proved through the measurement of the fluorescence signal produced by the labeled sample. Introducing PCFs instead of glass chips can lead to a significant improvement of the sensitivity, with respect to the present technology. DNA sensors based in HC-PCFs were reported: by using a highly efficient evanescent-wave detection of fluorophore-labeled biomolecule in aqueous solutions positioned in the air holes of the microstructured part of the PCF [185] or by using 16 mm long piece of functionalized HC-PCF incorporated into an optic-fluidic coupler chip towards the capture of a specific single-stranded DNA string by immobilizing a sensing layer on the microstructured internal surfaces of the fiber [186]. Using solid core PCF Bragg grating the detection of selected single-stranded DNA molecules was reported, being hybridized to a biofilm in the air holes of the PCF, measuring their interaction with the fiber modes [187]. By using LPGs in an LMA PCF and immobilizing a layer of biomolecules on the sides of the holes of the PCF, the thickness of double-stranded DNA was measured [188]. A biosensor for DNA detection based in a three-hole SCF was demonstrated, by functionalization and selective detection of DNA through hybridization of immobilized peptide nucleic acid probes [189].

Protein Sensors. Detection of specific protein entails the immobilization of antibodies for selective binding of antigens to antibodies and/or fluorescent labeling such proteins. Detection of quantum-dot-labeled proteins was reported using a soft-glass three-hole SCF and near-infrared light. The protein concentration was measured using this fluorescence capture approach, with a detection limit of 1 nM and extremely small sample volume (of order of 10 pl) [190]. The rendering of biologically active three-hole glass SCF via immobilization of antibodies within the holes of the fiber cross-section was demonstrated for detection of proteins [191]. The recognition of the proteins that bind to the antibodies is made through fluorescence labeling, opening up the possibility for measurement of multiple biomolecules via immobilization of multiple antibodies.

Other Molecular Sensors. Water molecules can be detected through their stretching vibrations-related Raman resonance. This detection was verified in the spectrum of an FWM signal of a, HC-PCF filled with water, suggesting phase-matched coherent anti-Stokes Raman scattering in inner fiber walls [192, 193]. Using Raman spectroscopy, different synthesis stages of ZnO nanoparticles inside a HC-PCF can be observed using very low pump powers [194]. Different synthesis stages can be differentiated through the Raman modes obtained using concentrations lower than 1% due to the high light/sample overlap. The detection of thiocyanate anions, with a sensitivity of 1.7×10^{-7} M, as well as water and ethanol was demonstrated by filling the hollow-core of a PCF and measuring the trace volume using SERS and a small volume of ~0.1 μL [195]. Using SERS in a solid core PCF with silver nanoparticles cluster the detection of 4-mercaptobenzoic acid was reported [196]. Evanescent-field sensing is a very used technique in molecular detection: inserting Methylene Blue in the cladding holes of a solid core PCF its absorption spectrum was measured [197] and its catalytic reactions monitored the a hollow core of a kagome PCF [198]; by filling the three-holes of a SCF, an aqueous NiCl2 solution absorption was measured [199]; by filling the cladding holes of a solid core PCF with cobalt chloride, its concentration variations were detected through absorption spectroscopy with a sensitivity of $1.6\,\mathrm{M}^{-1}$ [200]. A salinity sensor was also developed using a polyimide-coated Hi-Bi PCF Sagnac interferometer based on coating-induced radial swelling [201]. This sensor achieved a salinity sensitivity of 0.742 nm/(mol/L), which implies 45 times more sensitivity than that of a polyimide-coated FBG.

3.2.3. Humidity and pH Sensors. Humidity measurement is required for several applications, including meteorological services, chemical and food processing industry, civil engineering, air-conditioning, horticulture and electronic processing. OFs humidity sensors offer unique advantages, such as small size and weight, immunity to electromagnetic interference, corrosion resistance and remote operation, when compared with their electronic counterparts. Most of fiber optics humidity sensors work on the basis of a hygroscopic material coated over it to modulate the light propagating through the fiber. A humidity sensor was developed through the use of an LMA PCF-based interferometer operating in reflection, without the use of any hygroscopic material, with a sensitivity of 5.6–24 pm/% RH [202].

Another parameter that is important to monitor is pH. For application fields such as medicine, environmental sciences, agriculture, food science, or biotechnology the screen of pH is an important concern. PCF as a pH-sensing probe is endowed with the advantages of being flexible, the air-hole microstructure greatly enhances the specific surface area for sensing, and given that the sensing process is carried out in the air holes microanalysis is possible. A pH sensor was demonstrated based on a pH-sensitive fluorescence dye-doped cellulose acetate thin-film modified polymer PCF [203], showing the possibility to tailor the pH response range through doping a surfactant in the sensing film.

4. Technology Development Opportunities

Photonic crystal fiber-based sensing technology is still at its youth when compared to fields such as supercontinuum generation. The first sensor developed based in a photonic crystal fiber appeared in 2000, and since then an exponential growth on the number of publications in this field was observed. The interest of the scientific community in using photonic crystal fibers as sensing elements took this research field to flare up, but not yet enough as to lead it to

commercialization. Nevertheless, the perspectives to achieve commercial availability of sensing solutions based in these fibers are optimistic. Several authors have obtained patents for sensors based in photonic crystal fibers. The area of bio chemical sensing is the one with more patents using PCFs: for the detection of adsorbates on the interior surfaces of the PCF air holes [204]; by the functionalization of the air holes in the cladding of the PCF for detection of chemical and biological agents through SERS [205]; by using half HC-PCF adjacent to a surface of an optical waveguide layer of a substrate, an analyte can be inserted in the half-core of the PCF in order to be identified by a spectroscopy interaction [206]; via taking advantage of a hollow core photonic crystal fiber as a Raman biosensor [207]; by filling the hollow core of a PCF with SERS substrate and analyte for chemical and biological detection [208, 209]; or even by producing a resonator using a solid core photonic crystal fiber coil to quantify an analyte [210, 211]. Temperature sensing with PCFs also has some patents: temperature measurement was developed by filling the fiber with a temperature-sensitive fluid [212] or accordingly with its fluorescent characteristic [213] and, even more, by using Hi-Bi PCF Sagnac loop mirrors with a partial perfusion [214] or with a PCF long-period grating differential demodulation [215]. Humidity sensors patents based on tapered and perfuse PCFs [216] and on injection-type PCFs [217] were also developed. Patents were completed for a PCF refractive index sensor based on polarization interference [218], as well as for a real-time measurement of fluid flow concentration based in a PCF [219]. An all-fiber liquid level sensor patented based in a PCF was also obtained [220], as it was a stress sensor based on a Hi-Bi PCF Sagnac loop mirror [221] and a current sensor through a photonic crystal fiber Bragg grating [222]. A hollow-core PCF was used for a Fabry-Perot interferometer in order to obtain a displacement sensor patent [223]; and a multiparameter sensor patent was completed based in a PCF [224]. In addition, patents using PCFs to construct gyroscopes were also attained: using different PCFs [225] or using a hollow-core PCF [226]. The number and content of patents based on PCFs is growing through the years, showing an open possibility for future commercial exploitation.

5. Conclusions and Final Remarks

The diversity of unusual features of photonic crystal fibers, beyond what conventional fibers can offer, leads to an increase of possibilities for new and improved sensors. There is a huge interest of the scientific community in this original technology for applications in a variety of fields. Physical sensing is the more developed area of application so far, with a vast field of published fiber sensors. There are not so many developed sensors in the bio chemical field, but progress is shown in that direction. Several more sensors are expected to be developed for applications in this area due to the noteworthy characteristics photonic crystal fibers can offer. The amount and quality of photonic crystal fiber sensors developed nowadays, and presented in this paper, show that photonic crystal fiber is a technology with an outstanding potential for sensing applications. This potential can be further seen in the amount of existent patents of photonic crystal fiber sensors, which unlock the path for a commercial scenario.

The photonic crystal fibers sensing is a field that is growing by the day, and as so, it was not possible to mention every publication or patent or every detail of each sensor. Nevertheless, the overall assessment of photonic crystal fiber-based sensing and the possibilities offered by these fibers were presented, showing their valuable contribution to optical sensing technology.

List of Acronyms

ESM: Endlessly single mode
FBG: Fiber bragg grating
FP: Fabry-Perot
FWM: Four wave mixing
Hi-Bi: Highly birefringent
HC: Hollow-core
LC: Liquid crystal
LMA: Large-mode area
LPG: Long-period grating
MZI: Mach-Zehnder interferometer
MMF: Multimode fiber
OF: Optical fiber
PBG: Photonic bandgap
PBF: Photonic bandgap fiber
PCF: Photonic crystal fiber
RIU: Refractive index units
SCF: Suspended-core fiber
SERS: Surface-enhanced raman scattering
SMF: Single mode fiber
SPR: Surface plasmon resonance
TIR: Total internal reflection.

Acknowledgment

The authors are grateful to the Spanish Government project TEC2010-20224-C02-01.

References

[1] K. T. V. Grattan and T. Sun, "Fiber optic sensor technology: an overview," *Sensors and Actuators A*, vol. 82, no. 1, pp. 40–61, 2000.

[2] P. Russell, "Applied physics: photonic crystal fibers," *Science*, vol. 299, no. 5605, pp. 358–362, 2003.

[3] P. R. Laurent Bigot and P. Roy, "Fibres à cristal photonique: 10 ans d'existence et un vaste champ d'applications," *Images de la physique*, pp. 71–80, 2007.

[4] S. Arismar Cerqueira, "Recent progress and novel applications of photonic crystal fibers," *Reports on Progress in Physics*, vol. 73, no. 2, Article ID 024401, 2010.

[5] J. C. Knight, T. A. Birks, P. S. J. Russell, and D. M. Atkin, "All-silica single-mode optical fiber with photonic crystal cladding," *Optics Letters*, vol. 21, no. 19, pp. 1547–1549, 1996.

[6] J. C. Knight, T. A. Birks, R. F. Cregan, P. S. J. Russell, and J. P. De Sandro, "Large mode area photonic crystal fibre," *Electronics Letters*, vol. 34, no. 13, pp. 1347–1348, 1998.

[7] C. Lecaplain, B. Ortaç, G. MacHinet et al., "High-energy femtosecond photonic crystal fiber laser," *Optics Letters*, vol. 35, no. 19, pp. 3156–3158, 2010.

[8] D. Chen and L. Shen, "Switchable and tunable erbium-doped fiber ring laser incorporating a birefringent and highly nonlinear photonic crystal fiber," *Laser Physics Letters*, vol. 4, no. 5, pp. 368–370, 2007.

[9] A. M. R. Pinto, O. Frazão, J. L. Santos, and M. López-Amo, "Multiwavelength Raman fiber lasers using Hi-Bi photonic crystal fiber loop mirrors combined with random cavities," *Journal of Lightwave Technology*, vol. 29, no. 10, Article ID 5740550, pp. 1482–1488, 2011.

[10] G. Kakarantzas, T. A. Birks, and P. S. J. Russell, "Structural long-period gratings in photonic crystal fibers," *Optics Letters*, vol. 27, no. 12, pp. 1013–1015, 2002.

[11] J. M. Dudley, G. Genty, and S. Coen, "Supercontinuum generation in photonic crystal fiber," *Reviews of Modern Physics*, vol. 78, no. 4, pp. 1135–1184, 2006.

[12] G. Humbert, W. J. Wadsworth, S. G. Leon-Saval et al., "Supercontinuum generation system for optical coherence tomography based on tapered photonic crystal fibre," *Optics Express*, vol. 14, no. 4, pp. 1596–1603, 2006.

[13] R. Holzwarth, T. Udem, T. W. Hänsch, J. C. Knight, W. J. Wadsworth, and P. S. J. Russell, "Optical frequency synthesizer for precision spectroscopy," *Physical Review Letters*, vol. 85, no. 11, pp. 2264–2267, 2000.

[14] O. Frazão, J. L. Santos, F. M. Araújo, and L. A. Ferreira, "Optical sensing with photonic crystal fibers," *Laser and Photonics Reviews*, vol. 2, no. 6, pp. 449–459, 2008.

[15] P. S. J. Russell, "Photonic-crystal fibers," *Journal of Lightwave Technology*, vol. 24, no. 12, pp. 4729–4749, 2006.

[16] R. F. Cregan, B. J. Mangan, J. C. Knight et al., "Single-mode photonic band gap guidance of light in air," *Science*, vol. 285, no. 5433, pp. 1537–1539, 1999.

[17] D. G. Ouzounov, F. R. Ahmad, D. Müller et al., "Generation of megawatt optical solitons in hollow-core photonic band-gap fibers," *Science*, vol. 301, no. 5640, pp. 1702–1704, 2003.

[18] F. Benabid, J. C. Knight, G. Antonopoulos, and P. S. J. Russell, "Stimulated Raman scattering in hydrogen-filled hollow-core photonic crystal fiber," *Science*, vol. 298, no. 5592, pp. 399–402, 2002.

[19] S. Ghosh, J. E. Sharping, D. G. Ouzounov, and A. L. Gaeta, "Resonant optical interactions with molecules confined in photonic band-gap fibers," *Physical Review Letters*, vol. 94, no. 9, Article ID 093902, 2005.

[20] F. Benabid, J. C. Knight, and P. S. J. Russell, "Particle levitation and guidance in hollow-core photonic crystal fiber," *Optics Express*, vol. 10, no. 21, pp. 1195–1203, 2002.

[21] T. G. Euser, M. K. Garbos, J. S. Y. Chen, and P. S. J. Russell, "Precise balancing of viscous and radiation forces on a particle in liquid-filled photonic bandgap fiber," *Optics Letters*, vol. 34, no. 23, pp. 3674–3676, 2009.

[22] W. Jin, H. F. Xuan, and H. L. Ho, "Sensing with hollow-core photonic bandgap fibers," *Measurement Science and Technology*, vol. 21, no. 9, Article ID 094014, 2010.

[23] V. V. Tuchin, Y. S. Skibina, V. I. Beloglazov et al., "Sensor properties of hollow-core photonic crystal fibers," *Technical Physics Letters*, vol. 34, no. 8, pp. 663–665, 2008.

[24] J. M. Lopez-Higuera, L. Rodriguez Cobo, A. Quintela Incera, and A. Cobo, "Fiber optic sensors in structural health monitoring," *IEEE Journal of Lightwave Technology*, vol. 29, no. 4, pp. 587–608, 2011.

[25] H. N. Li, D. S. Li, and G. B. Song, "Recent applications of fiber optic sensors to health monitoring in civil engineering," *Engineering Structures*, vol. 26, no. 11, pp. 1647–1657, 2004.

[26] C. Sonnenfeld, S. Sulejmani, T. Geernaert et al., "Microstructured optical fiber sensors embedded in a laminate composite for smart material applications," *Sensors*, vol. 11, no. 3, pp. 2566–2579, 2011.

[27] B. Culshaw, "Fiber optics in sensing and measurement," *IEEE Journal on Selected Topics in Quantum Electronics*, vol. 6, no. 6, pp. 1014–1021, 2000.

[28] P. M. Blanchard, J. G. Burnett, G. R. G. Erry et al., "Two-dimensional bend sensing with a single, multi-core optical fibre," *Smart Materials and Structures*, vol. 9, no. 2, pp. 132–140, 2000.

[29] W. N. MacPherson, M. J. Gander, R. McBride et al., "Remotely addressed optical fibre curvature sensor using multi-core photonic crystal fibre," *Optics Communications*, vol. 193, no. 1–6, pp. 97–104, 2001.

[30] J. Villatoro, V. Finazzi, G. Badenes, and V. Pruneri, "Highly sensitive sensors based on photonic crystal fiber modal interferometers," *Journal of Sensors*, vol. 2009, Article ID 747803, 2009.

[31] O. Frazão, J. Baptista, J. L. Santos, and P. Roy, "Curvature sensor using a highly birefringent photonic crystal fiber with two asymmetric hole regions in a Sagnac interferometer," *Applied Optics*, vol. 47, no. 13, pp. 2520–2523, 2008.

[32] H. P. Gong, C. C. Chan, P. Zu, L. H. Chen, and X. Y. Dong, "Curvature measurement by using low-birefringence photonic crystal fiber based Sagnac loop," *Optics Communications*, vol. 283, no. 16, pp. 3142–3144, 2010.

[33] W. C. Wong, C. C. Chan, H. Gong, and K. C. Leong, "Mach-Zehnder photonic crystal interferometer in cavity ring-down loop for curvature measurement," *IEEE Photonics Technology Letters*, vol. 23, no. 12, pp. 795–797, 2011.

[34] M. Deng, C. P. Tang, T. Zhu, and Y. J. Rao, "Highly sensitive bend sensor based on Mach-Zehnder interferometer using photonic crystal fiber," *Optics Communications*, vol. 284, no. 12, pp. 2849–2853, 2011.

[35] B. Dong, J. Hao, and Z. Xu, "Temperature insensitive curvature measurement with a core-offset polarization maintaining photonic crystal fiber based interferometer," *Optical Fiber Technology*, vol. 17, no. 3, pp. 233–235, 2011.

[36] H. Dobb, K. Kalli, and D. J. Webb, "Temperature-insensitive long period grating sensors in photonic crystal fibre," *Electronics Letters*, vol. 40, no. 11, pp. 657–658, 2004.

[37] Z. He, Y. Zhu, and H. Du, "Effect of macro-bending on resonant wavelength and intensity of long-period gratings in photonic crystal fiber," *Optics Express*, vol. 15, no. 4, pp. 1804–1810, 2007.

[38] T. Allsop, K. Kalli, K. Zhou et al., "Long period gratings written into a photonic crystal fibre by a femtosecond laser as directional bend sensors," *Optics Communications*, vol. 281, no. 20, pp. 5092–5096, 2008.

[39] L. Jin, W. Jin, and J. Ju, "Directional bend sensing with a co_2 long period grating in a photonic crystal fiber," *Journal of Lightwave Technology*, vol. 27, no. 21, pp. 4884–4891, 2009.

[40] Y. G. Han, "Temperature-insensitive strain measurement using a birefringent interferometer based on a polarization-maintaining photonic crystal fiber," *Applied Physics B*, vol. 95, no. 2, pp. 383–387, 2009.

[41] J. Villatoro, V. P. Minkovich, and D. Monzón-Hernández, "Temperature-independent strain sensor made from tapered holey optical fiber," *Optics Letters*, vol. 31, no. 3, pp. 305–307, 2006.

[42] J. Villatoro, V. P. Minkovich, and D. Monzón-Hernández, "Compact modal interferometer built with tapered microstructured optical fiber," *IEEE Photonics Technology Letters*, vol. 18, no. 11, pp. 1258–1260, 2006.

[43] J. Villatoro, V. Finazzi, V. P. Minkovich, V. Pruneri, and G. Badenes, "Temperature-insensitive photonic crystal fiber interferometer for absolute strain sensing," *Applied Physics Letters*, vol. 91, no. 9, Article ID 091109, 2007.

[44] B. Dong and E. J. Hao, "Temperature-insensitive and intensity-modulated embedded photonic-crystal-fiber modal-interferometer-based microdisplacement sensor," *Journal of the Optical Society of America B*, vol. 28, no. 10, pp. 2332–2336, 2011.

[45] Q. Shi, F. Y. Lv, Z. Wang et al., "Environmentally stable Fabry-Perot-type strain sensor based on hollow-core photonic bandgap fiber," *IEEE Photonics Technology Letters*, vol. 20, no. 4, pp. 237–239, 2008.

[46] Q. Shi, Z. Wang, L. Jin et al., "A hollow-core photonic crystal fiber cavity based multiplexed Fabry-Perot interferometric strain sensor system," *IEEE Photonics Technology Letters*, vol. 20, no. 15, pp. 1329–1331, 2008.

[47] O. Frazao, J. M. Baptista, and J. L. Santos, "Temperature-independent strain sensor based on a Hi-Bi photonic crystal fiber loop mirror," *IEEE Sensors Journal*, vol. 7, no. 10, pp. 1453–1455, 2007.

[48] W. Qian, C. L. Zhao, X. Dong, and W. Jin, "Intensity measurement based temperature-independent strain sensor using a highly birefringent photonic crystal fiber loop mirror," *Optics Communications*, vol. 283, no. 24, pp. 5250–5254, 2010.

[49] H. Zhang, B. Liu, Z. Wang et al., "Temperature-insensitive displacement sensor based on high-birefringence photonic crystal fiber loop mirror," *Optica Applicata*, vol. 40, no. 1, pp. 209–217, 2010.

[50] M. Bravo, A. M. R. Pinto, M. Lopez-Amo, J. Kobelke, and K. Schuster, "High precision micro-displacement fiber sensor through a suspended-core Sagnac interferometer," *Optics Letters*, vol. 37, no. 2, pp. 202–204, 2012.

[51] W. Zhou, W. C. Wong, C. C. Chan, L. Y. Shao, and X. Dong, "Highly sensitive fiber loop ringdown strain sensor using photonic crystal fiber interferometer," *Applied Optics*, vol. 50, no. 19, pp. 3087–3092, 2011.

[52] S. Mathews, G. Farrell, and Y. Semenova, "All-fiber polarimetric electric field sensing using liquid crystal infiltrated photonic crystal fibers," *Sensors and Actuators A*, vol. 167, no. 1, pp. 54–59, 2011.

[53] T. R. Wolinski, K. Szaniawska, S. Ertman et al., "Influence of temperature and electrical fields on propagation properties of photonic liquid-crystal fibres," *Measurement Science and Technology*, vol. 17, no. 5, pp. 985–991, 2006.

[54] T. R. Wolinski, A. Czapla, S. Ertman et al., "Photonic liquid crystal fibers for sensing applications," *IEEE Transactions on Instrumentation and Measurement*, vol. 57, no. 8, pp. 1796–1802, 2008.

[55] S. Mathews, G. Farrell, and Y. Semenova, "Directional electric field sensitivity of a liquid crystal infiltrated photonic crystal fiber," *IEEE Photonics Technology Letters*, vol. 23, no. 7, pp. 408–410, 2011.

[56] S. Mathews, G. Farrell, and Y. Semenova, "Liquid crystal infiltrated photonic crystal fibers for electric field intensity measurements," *Applied Optics*, vol. 50, no. 17, pp. 2628–2635, 2011.

[57] A. Michie, J. Canning, I. Bassett et al., "Spun elliptically birefringent photonic crystal fibre for current sensing," *Measurement Science and Technology*, vol. 18, no. 10, pp. 3070–3074, 2007.

[58] Y. K. Chamorovskiy, N. I. Starostin, M. V. Ryabko et al., "Miniature microstructured fiber coil with high magneto-optical sensitivity," *Optics Communications*, vol. 282, no. 23, pp. 4618–4621, 2009.

[59] H. V. Thakur, S. M. Nalawade, S. Gupta, R. Kitture, and S. N. Kale, "Photonic crystal fiber injected with Fe_3O_4 nanofluid for magnetic field detection," *Applied Physics Letters*, vol. 99, Article ID 161101, 3 pages, 2011.

[60] S. M. M. Quintero, C. Martelli, A. M. B. Braga, L. C. G. Valente, and C. C. Kato, "Magnetic field measurements based on terfenol coated photonic crystal fibers," *Sensors*, vol. 11, no. 12, pp. 11103–11111, 2011.

[61] Y. Zhao, R. Q. Lv, Y. Ying, and Q. Wang, "Hollow-core photonic crystal fiber Fabry-Perot sensor for magnetic field measurement based on magnetic fluid," *Optics and Laser Technology*, vol. 44, pp. 899–902, 2012.

[62] W. J. Bock, J. Chen, P. Mikulic, T. Eftimov, and M. Korwin-Pawlowski, "Pressure sensing using periodically tapered long-period gratings written in photonic crystal fibres," *Measurement Science and Technology*, vol. 18, no. 10, pp. 3098–3102, 2007.

[63] W. J. Bock, J. Chen, T. Eftimov, and W. Urbanczyk, "A photonic crystal fiber sensor for pressure measurements," *IEEE Transactions on Instrumentation and Measurement*, vol. 55, no. 4, pp. 1119–1123, 2006.

[64] H. K. Gahir and D. Khanna, "Design and development of a temperature-compensated fiber optic polarimetric pressure sensor based on photonic crystal fiber at 1550 nm," *Applied Optics*, vol. 46, no. 8, pp. 1184–1189, 2007.

[65] F. C. Fávero, S. M. M. Quintero, C. Martelli et al., "Hydrostatic pressure sensing with high birefringence photonic crystal fibers," *Sensors*, vol. 10, no. 11, pp. 9698–9711, 2010.

[66] Y. S. Shinde and H. K. Gahir, "Dynamic pressure sensing study using photonic crystal fiber: application to tsunami sensing," *IEEE Photonics Technology Letters*, vol. 20, no. 4, pp. 279–281, 2008.

[67] T. Nasilowski, T. Martynkien, G. Statkiewicz et al., "Temperature and pressure sensitivities of the highly birefringent photonic crystal fiber with core asymmetry," *Applied Physics B*, vol. 81, no. 2-3, pp. 325–331, 2005.

[68] T. Martynkien, M. Szpulak, G. Statkiewicz et al., "Measurements of sensitivity to hydrostatic pressure and temperature in highly birefringent photonic crystal fibers," *Optical and Quantum Electronics*, vol. 39, no. 4–6, pp. 481–489, 2007.

[69] T. Martynkien, G. Statkiewicz-Barabach, J. Olszewski et al., "Highly birefringent microstructured fibers with enhanced sensitivity to hydrostatic pressure," *Optics Express*, vol. 18, no. 14, pp. 15113–15121, 2010.

[70] H. Y. Fu, H. Y. Tam, L. Y. Shao et al., "Pressure sensor realized with polarization-maintaining photonic crystal fiber-based Sagnac interferometer," *Applied Optics*, vol. 47, no. 15, pp. 2835–2839, 2008.

[71] H. Y. Fu, C. Wu, M. L. V. Tse et al., "High pressure sensor based on photonic crystal fiber for downhole application," *Applied Optics*, vol. 49, no. 14, pp. 2639–2643, 2010.

[72] S. H. Aref, M. I. Zibaii, M. Kheiri et al., "Pressure and temperature characterization of two interferometric configurations based on suspended-core fibers," *Optics Communications*, vol. 285, no. 3, pp. 269–273, 2012.

[73] T. Martynkien, M. Szpulak, and W. Urbanczyk, "Modeling and measurement of temperature sensitivity in birefringent photonic crystal holey fibers," *Applied Optics*, vol. 44, no. 36, pp. 7780–7788, 2005.

[74] J. Ju, Z. Wang, W. Jin, and M. S. Demokan, "Temperature sensitivity of a two-mode photonic crystal fiber interferometric sensor," *IEEE Photonics Technology Letters*, vol. 18, no. 20, pp. 2168–2170, 2006.

[75] D. Monzon-Hernandez, V. P. Minkovich, and J. Villatoro, "High-temperature sensing with tapers made of microstructured optical fiber," *IEEE Photonics Technology Letters*, vol. 18, no. 3, pp. 511–513, 2006.

[76] S. S. Li, Z. D. Huang, X. S. Song et al., "Photonic crystal fibre based high temperature sensor with three-beam path interference," *Electronics Letters*, vol. 46, no. 20, pp. 1394–1396, 2010.

[77] S. M. Nalawade and H. V. Thakur, "Photonic crystal fiber strain-independent temperature sensing based on modal interferometer," *IEEE Photonics Technology Letters*, vol. 23, no. 21, pp. 1600–1602, 2011.

[78] J. Ju, W. Jin, and H. L. Ho, "Compact in-fiber interferometer formed by long-period gratings in photonic crystal fiber," *IEEE Photonics Technology Letters*, vol. 20, no. 23, pp. 1899–1901, 2008.

[79] Y. Geng, X. Li, X. Tan, Y. Deng, and Y. Yu, "Sensitivity-enhanced high-temperature sensing using all-solid photonic bandgap fiber modal interference," *Applied Optics*, vol. 50, no. 4, pp. 468–472, 2011.

[80] H. Y. Choi, K. S. Pack, S. J. Park, U. C. Paek, B. H. Lee, and E. S. Choi, "Miniature fiber-optic high temperature sensor based on a hybrid structured Fabry-Perot interferometer," *Optics Letters*, vol. 33, no. 21, pp. 2455–2457, 2008.

[81] A. M. R. Pinto, O. Frazão, J. L. Santos, M. Lopez-Amo, J. Kobelke, and K. Schuster, "Interrogation of a suspended-core Fabry-Perot temperature sensor through a dual wavelength Raman fiber laser," *Journal of Lightwave Technology*, vol. 28, no. 21, Article ID 5582123, pp. 3149–3155, 2010.

[82] A. M. R. Pinto, M. Lopez-Amo, J. Kobelke, and K. Schuster, "Temperature fiber laser sensor based on a hybrid cavity and a random mirror," *IEEE Journal of Lightwave Technology*, no. 99, 2011.

[83] Y. Zhu, P. Shum, H. W. Bay et al., "Strain-insensitive and high-temperature long-period gratings inscribed in photonic crystal fiber," *Optics Letters*, vol. 30, no. 4, pp. 367–369, 2005.

[84] B. H. Kim, S. H. Lee, A. Lin, C. L. Lee, J. Lee, and W. T. Han, "Large temperature sensitivity of Sagnac loop interferometer based on the birefringent holey fiber filled with metal indium," *Optics Express*, vol. 17, no. 3, pp. 1789–1794, 2009.

[85] W. Qian, C. L. Zhao, S. He et al., "High-sensitivity temperature sensor based on an alcohol-filled photonic crystal fiber loop mirror," *Optics Letters*, vol. 36, no. 9, pp. 1548–1550, 2011.

[86] B. Larrion, M. Hernandez, F. J. Arregui, J. Goicoechea, J. Bravo, and I. R. Matias, "Photonic crystal fiber temperature sensor based on quantum dot nanocoatings," *Journal of Sensors*, vol. 2009, Article ID 932471, 6 pages, 2009.

[87] A. Bozolan, R. M. Gerosa, C. J. S. de Matos, and M. A. Romero, "Temperature sensing using colloidal-core photonic crystal fiber," *IEEE Sensors Journal*, vol. 12, no. 1, pp. 195–200, 2012.

[88] Y. Miao, B. Liu, K. Zhang, Y. Liu, and H. Zhang, "Temperature tunability of photonic crystal fiber filled with fe_3o_4 nanoparticle fluid," *Applied Physics Letters*, vol. 98, no. 2, Article ID 021103, 2011.

[89] Y. Yu, X. Li, X. Hong et al., "Some features of the photonic crystal fiber temperature sensor with liquid ethanol filling," *Optics Express*, vol. 18, no. 15, pp. 15383–15388, 2010.

[90] W. Ying, Y. Minwei, D. N. Wang, and C. R. Liao, "Selectively infiltrated photonic crystal fiber with ultrahigh temperature sensitivity," *IEEE Photonics Technology Letters*, vol. 23, no. 20, pp. 1520–1522, 2011.

[91] L. Zou, X. Bao, and L. Chen, "Distributed Brillouin temperature sensing in photonic crystal fiber," *Smart Materials and Structures*, vol. 14, no. 3, pp. S8–S11, 2005.

[92] Y. Dong, X. Bao, and L. Chen, "Distributed temperature sensing based on birefringence effect on transient Brillouin grating in a polarization-maintaining photonic crystal fiber," *Optics Letters*, vol. 34, no. 17, pp. 2590–2592, 2009.

[93] H. Y. Fu, S. K. Khijwania, H. Y. Tam, P. K. A. Wai, and C. Lu, "Polarization-maintaining photonic-crystal-fiber-based all-optical polarimetric torsion sensor," *Applied Optics*, vol. 49, no. 31, pp. 5954–5958, 2010.

[94] O. Frazao, C. Jesus, J. M. Baptista, J. L. Santos, and P. Roy, "Fiber-optic interferometric torsion sensor based on a two-lp-mode operation in birefringent fiber," *IEEE Photonics Technology Letters*, vol. 21, no. 17, pp. 1277–1279, 2009.

[95] H. M. Kim, T. H. Kim, B. Kim, and Y. Chung, "Temperature-insensitive torsion sensor with enhanced sensitivity by use of a highly birefringent photonic crystal fiber," *IEEE Photonics Technology Letters*, vol. 22, no. 20, pp. 1539–1541, 2010.

[96] W. G. Chen, S. Q. Lou, L. W. Wang, H. Zou, W. L. Lu, and S. S. Jian, "Highly sensitive torsion sensor based on Sagnac interferometer using side-leakage photonic crystal fiber," *IEEE Photonics Technology Letters*, vol. 23, no. 21, pp. 1639–1641, 2011.

[97] P. Zu, C. C. Chan, Y. Jin et al., "A temperature-insensitive twist sensor by using low-birefringence photonic-crystal-fiber-based Sagnac interferometer," *IEEE Photonics Technology Letters*, vol. 23, no. 13, pp. 920–922, 2011.

[98] X. Yu, P. Shum, S. Fu, and L. Deng, "Torsion-sensitivity of mechanical long-period grating in photonic crystal fiber," *Journal of Optoelectronics and Advanced Materials*, vol. 8, no. 3, pp. 1247–1249, 2006.

[99] D. E. Ceballos-Herrera, I. Torres-Gomez, A. Martinez-Rios, L. Garcia, and J. J. Sanchez-Mondragon, "Torsion sensing characteristics of mechanically induced long-period holey fiber gratings," *IEEE Sensors Journal*, vol. 10, no. 7, pp. 1200–1205, 2010.

[100] H. M. Kim, T. H. Kim, B. Kim, and Y. Chung, "Enhanced transverse load sensitivity by using a highly birefringent photonic crystal fiber with larger air holes on one axis," *Applied Optics*, vol. 49, no. 20, pp. 3841–3845, 2010.

[101] C. Jewart, K. P. Chen, B. McMillen et al., "Sensitivity enhancement of fiber bragg gratings to transverse stress by using microstructural fibers," *Optics Letters*, vol. 31, no. 15, pp. 2260–2262, 2006.

[102] T. Geernaert, G. Luyckx, E. Voet et al., "Transversal load sensing with fiber bragg gratings in microstructured optical fibers," *IEEE Photonics Technology Letters*, vol. 21, no. 1, pp. 6–8, 2009.

[103] Y. Wang, H. Bartelt, W. Ecke et al., "Investigating transverse loading characteristics of microstructured fiber bragg gratings with an active fiber depolarizer," *IEEE Photonics Technology Letters*, vol. 21, no. 19, pp. 1450–1452, 2009.

[104] C. M. Jewart, T. Chen, E. Lindner et al., "Suspended-core fiber bragg grating sensor for directional-dependent transverse stress monitoring," *Optics Letters*, vol. 36, no. 12, pp. 2360–2362, 2011.

[105] C. F. Fan, C. L. Chiang, and C. P. Yu, "Birefringent photonic crystal fiber coils and their application to transverse

displacement sensing," *Optics Express*, vol. 19, no. 21, pp. 19948–19954, 2011.

[106] P. Zu, C. C. Chan, Y. Jin, Y. Zhang, and X. Dong, "Fabrication of a temperature-insensitive transverse mechanical load sensor by using a photonic crystal fiber-based Sagnac loop," *Measurement Science and Technology*, vol. 22, no. 2, Article ID 025204, 2011.

[107] M. C. P. Huy, G. Laffont, V. Dewynter et al., "Three-hole microstructured optical fiber for efficient fiber bragg grating refractometer," *Optics Letters*, vol. 32, no. 16, pp. 2390–2392, 2007.

[108] C. Martelli, J. Canning, M. Kristensen, and N. Groothoff, "Refractive index measurement within a photonic crystal fibre based on short wavelength diffraction," *Sensors*, vol. 7, no. 11, pp. 2492–2498, 2007.

[109] Y. Zhu, Z. He, and H. Du, "Detection of external refractive index change with high sensitivity using long-period gratings in photonic crystal fiber," *Sensors and Actuators B*, vol. 131, no. 1, pp. 265–269, 2008.

[110] Z. He, F. Tian, Y. Zhu, N. Lavlinskaia, and H. Du, "Long-period gratings in photonic crystal fiber as an optofluidic label-free biosensor," *Biosensors and Bioelectronics*, vol. 26, no. 12, pp. 4774–4778, 2011.

[111] Z. He, Y. Zhu, and H. Du, "Long-period gratings inscribed in air- and water-filled photonic crystal fiber for refractometric sensing of aqueous solution," *Applied Physics Letters*, vol. 92, no. 4, Article ID 044105, 2008.

[112] L. Rindorf and O. Bang, "Highly sensitive refractometer with a photonic-crystal-fiber long-period grating," *Optics Letters*, vol. 33, no. 6, pp. 563–565, 2008.

[113] V. P. Minkovich, J. Villatoro, D. Monzón-Hernández, S. Calixto, A. B. Sotsky, and L. I. Sotskaya, "Holey fiber tapers with resonance transmission for high-resolution refractive index sensing," *Optics Express*, vol. 13, no. 19, pp. 7609–7614, 2005.

[114] D. Monzon-Hernandez, V. P. Minkovich, J. Villatoro, M. P. Kreuzer, and G. Badenes, "Photonic crystal fiber microtaper supporting two selective higher-order modes with high sensitivity to gas molecules," *Applied Physics Letters*, vol. 93, Article ID 081106, 3 pages, 2008.

[115] R. Jha, J. Villatoro, and G. Badenes, "Ultrastable in reflection photonic crystal fiber modal interferometer for accurate refractive index sensing," *Applied Physics Letters*, vol. 93, no. 19, Article ID 191106, 2008.

[116] D. K. C. Wu, B. T. Kuhlmey, and B. J. Eggleton, "Ultrasensitive photonic crystal fiber refractive index sensor," *Optics Letters*, vol. 34, no. 3, pp. 322–324, 2009.

[117] R. Jha, J. Villatoro, G. Badenes, and V. Pruneri, "Refractometry based on a photonic crystal fiber interferometer," *Optics Letters*, vol. 34, no. 5, pp. 617–619, 2009.

[118] S. Silva, J. L. Santos, F. X. Malcata, J. Kobelke, K. Schuster, and O. Frazao, "Optical refractometer based on large-core air-clad photonic crystal fibers," *Optics Letters*, vol. 36, no. 6, pp. 852–854, 2011.

[119] M. Smietana, D. Brabant, W. Bock, P. Mikulic, and T. Eftimov, "Refractive-index sensing with Inline core-cladding intermodal interferometer based on silicon nitride nanocoated photonic crystal fiber," *IEEE Journal of Lightwave Technology*, vol. 99, 2011.

[120] W. C. Wong, W. Zhou, C. C. Chan, X. Dong, and K. C. Leong, "Cavity ringdown refractive index sensor using photonic crystal fiber interferometer," *Sensors and Actuators B*, vol. 161, no. 1, pp. 108–113, 2011.

[121] M. H. Frosz, A. Stefani, and O. Bang, "Highly sensitive and simple method for refractive index sensing of liquids in microstructured optical fibers using four-wave mixing," *Optics Express*, vol. 19, no. 11, pp. 10471–10484, 2011.

[122] J. Sun and C. C. Chan, "Photonic bandgap fiber for refractive index measurement," *Sensors and Actuators B*, vol. 128, no. 1, pp. 46–50, 2007.

[123] X. Yu, P. Shum, G. B. Ren, and N. Q. Ngo, "Photonic crystal fibers with high index infiltrations for refractive index sensing," *Optics Communications*, vol. 281, no. 18, pp. 4555–4559, 2008.

[124] H. V. Thakur, S. M. Nalawade, Y. Saxena, and K. T. V. Grattan, "All-fiber embedded pm-pcf vibration sensor for structural health monitoring of composite," *Sensors and Actuators A*, vol. 167, no. 2, pp. 204–212, 2011.

[125] G. Rajan, M. Ramakrishnan, Y. Semenova et al., "Analysis of Vibration Measurements in a Composite Material Using an Embedded PM-PCF Polarimetric Sensor and an FBG Sensor," *IEEE Sensors Journal*, vol. 99, 2011.

[126] L. Zou, X. Bao, V. Shahraam Afshar, and L. Chen, "Dependence of the Brillouin frequency shift on strain and temperature in a photonic crystal fiber," *Optics Letters*, vol. 29, no. 13, pp. 1485–1487, 2004.

[127] Y. G. Han, Y. Chung, S. B. Lee, C. S. Kim, M. Y. Jeong, and M. K. Kim, "Temperature and strain discrimination based on a temperature-insensitive birefringent interferometer incorporating an erbium-doped fiber," *Applied Optics*, vol. 48, no. 12, pp. 2303–2307, 2009.

[128] C. Martelli, J. Canning, N. Groothoff, and K. Lyytikainen, "Strain and temperature characterization of photonic crystal fiber bragg gratings," *Optics Letters*, vol. 30, no. 14, pp. 1785–1787, 2005.

[129] O. Frazao, S. H. Aref, J. M. Baptista et al., "Fabry-Perot cavity based on a suspended-core fiber for strain and temperature measurement," *IEEE Photonics Technology Letters*, vol. 21, no. 17, pp. 1229–1231, 2009.

[130] Y. J. Rao, M. Deng, T. Zhu, and H. Li, "In-line Fabry-Perot etalons based on hollow-corephotonic bandgap fibers for high-temperature applications," *Journal of Lightwave Technology*, vol. 27, no. 19, pp. 4360–4365, 2009.

[131] O. Frazão, J. M. Baptista, J. L. Santos, J. Kobelke, and K. Schuster, "Strain and temperature characterisation of sensing head based on suspended-core fibre in Sagnac interferometer," *Electronics Letters*, vol. 44, no. 25, pp. 1455–1456, 2008.

[132] Y. G. Han, Y. Chung, and S. B. Lee, "Discrimination of strain and temperature based on a polarization-maintaining photonic crystal fiber incorporating an erbium-doped fiber," *Optics Communications*, vol. 282, no. 11, pp. 2161–2164, 2009.

[133] R. M. Andre, M. B. Marques, P. Roy, and O. Frazao, "Fiber loop mirror using a small core microstructured fiber for strain and temperature discrimination," *IEEE Photonics Technology Letters*, vol. 22, no. 15, pp. 1120–1122, 2010.

[134] G. Kim, T. Cho, K. Hwang et al., "Strain and temperature sensitivities of an elliptical hollow-core photonic bandgap fiber based on Sagnac interferometer," *Optics Express*, vol. 17, no. 4, pp. 2481–2486, 2009.

[135] O. Frazao, J. L. Santos, and J. M. Baptista, "Strain and temperature discrimination using IF concatenated high-birefringence fiber loop mirrors," *IEEE Photonics Technology Letters*, vol. 19, pp. 1260–1262, 2007.

[136] B. Gu, W. Yuan, S. He, and O. Bang, "Temperature compensated strain sensor based on cascaded Sagnac interferometers

and all-solid birefringent hybrid photonic crystal fibers," *IEEE Sensors Journal*, no. 99, 2011.

[137] S. H. Aref, R. Amezcua-Correa, J. P. Carvalho et al., "Modal interferometer based on hollow-core photonic crystal fiber for strain and temperature measurement," *Optics Express*, vol. 17, no. 21, pp. 18669–18675, 2009.

[138] G. Statkiewicz-Barabach, J. P. Carvalho, O. Frazão et al., "Intermodal interferometer for strain and temperature sensing fabricated in birefringent boron doped microstructured fiber," *Applied Optics*, vol. 50, no. 21, pp. 3742–3749, 2011.

[139] G. A. Cardenas-Sevilla, V. Finazzi, J. Villatoro, and V. Pruneri, "Photonic crystal fiber sensor array based on modes overlapping," *Optics Express*, vol. 19, no. 8, pp. 7596–7602, 2011.

[140] R. M. Silva, M. S. Ferreira, J. Kobelke, K. Schuster, and O. Frazao, "Simultaneous measurement of curvature and strain using a suspended multicore fiber," *Optics Letters*, vol. 36, no. 19, pp. 3939–3941, 2011.

[141] W. Shin, Y. L. Lee, B. A. Yu, Y. C. Noh, and T. J. Ahn, "Highly sensitive strain and bending sensor based on in-line fiber Mach-Zehnder interferometer in solid core large mode area photonic crystal fiber," *Optics Communications*, vol. 283, no. 10, pp. 2097–2101, 2010.

[142] G. Statkiewicz, T. Martynkien, and W. Urbańczyk, "Measurements of modal birefringence and polarimetric sensitivity of the birefringent holey fiber to hydrostatic pressure and strain," *Optics Communications*, vol. 241, no. 4–6, pp. 339–348, 2004.

[143] C. M. Jewart, Q. Wang, J. Canning, D. Grobnic, S. J. Mihailov, and K. P. Chen, "Ultrafast femtosecond-laser-induced fiber bragg gratings in air-hole microstructured fibers for high-temperature pressure sensing," *Optics Letters*, vol. 35, no. 9, pp. 1443–1445, 2010.

[144] T. Chen, R. Z. Chen, C. Jewart et al., "Regenerated gratings in air-hole microstructured fibers for high-temperature pressure sensing," *Optics Letters*, vol. 36, no. 18, pp. 3542–3544, 2011.

[145] J. Xu, Y. G. Liu, Z. Wang, and B. Tai, "Simultaneous force and temperature measurement using long-period grating written on the joint of a microstructured optical fiber and a single mode fiber," *Applied Optics*, vol. 49, no. 3, pp. 492–496, 2010.

[146] Y. J. Rao, M. Deng, D. W. Duan, and T. Zhu, "In-line fiber Fabry-Perot refractive-index tip sensor based on endlessly photonic crystal fiber," *Sensors and Actuators A*, vol. 148, no. 1, pp. 33–38, 2008.

[147] W. J. Bock, W. Urbanczyk, and J. Wojcik, "Measurements of sensitivity of the single-mode photonic crystal holey fibre to temperature, elongation and hydrostatic pressure," *Measurement Science and Technology*, vol. 15, no. 8, pp. 1496–1500, 2004.

[148] H. Dobb, K. Kalli, and D. J. Webb, "Measured sensitivity of arc-induced long-period grating sensors in photonic crystal fibre," *Optics Communications*, vol. 260, no. 1, pp. 184–191, 2006.

[149] O. Frazão, S. O. Silva, J. M. Baptista et al., "Simultaneous measurement of multiparameters using a Sagnac interferometer with polarization maintaining side-hole fiber," *Applied Optics*, vol. 47, no. 27, pp. 4841–4848, 2008.

[150] S. F. O. Silva, J. L. Santos, J. Kobelke, K. Schuster, and O. Frazao, "Simultaneous measurement of three parameters using an all-fiber Mach-Zehnder interferometer based on suspended twin-core fibers," *Optical Engineering*, vol. 50, Article ID 030501, 2011.

[151] O. S. Wolfbeis, "Fibre-optic sensors in biomedical sciences," *Pure and Applied Chemistry*, vol. 59, no. 5, pp. 663–672, 1987.

[152] M. Skorobogatiy, "Microstructured and photonic bandgap fibers for applications in the resonant bio- and chemical sensors," *Journal of Sensors*, vol. 2009, Article ID 524237, 2009.

[153] T. M. Monro, S. Warren-Smith, E. P. Schartner et al., "Sensing with suspended-core optical fibers," *Optical Fiber Technology*, vol. 16, no. 6, pp. 343–356, 2010.

[154] Y. L. Hoo, W. Jin, H. L. Ho, D. N. Wang, and R. S. Windeler, "Evanescent-wave gas sensing using microstructure fiber," *Optical Engineering*, vol. 41, no. 1, pp. 8–9, 2002.

[155] G. Pickrell, W. Peng, and A. Wang, "Random-hole optical fiber evanescent-wave gas sensing," *Optics Letters*, vol. 29, no. 13, pp. 1476–1478, 2004.

[156] A. S. Webb, F. Poletti, D. J. Richardson, and J. K. Sahu, "Suspended-core holey fiber for evanescent-field sensing," *Optical Engineering*, vol. 46, no. 1, Article ID 010503, 2007.

[157] G. F. Yan, A. P. Zhang, G. Y. Ma et al., "Fiber-optic acetylene gas sensor based on microstructured optical fiber bragg gratings," *IEEE Photonics Technology Letters*, vol. 23, no. 21, pp. 1588–1590, 2011.

[158] Y. L. Hoo, W. Jin, H. L. Ho, J. Ju, and D. N. Wang, "Gas diffusion measurement using hollow-core photonic bandgap fiber," *Sensors and Actuators B*, vol. 105, no. 2, pp. 183–186, 2005.

[159] R. Thapa, K. Knabe, M. Faheem, A. Naweed, O. L. Weaver, and K. L. Corwin, "Saturated absorption spectroscopy of acetylene gas inside large-core photonic bandgap fiber," *Optics Letters*, vol. 31, no. 16, pp. 2489–2491, 2006.

[160] E. Austin, A. van Brakel, M. N. Petrovich, and D. J. Richardson, "Fibre optical sensor for c_2h_2 gas using gas-filled photonic bandgap fibre reference cell," *Sensors and Actuators B*, vol. 139, no. 1, pp. 30–34, 2009.

[161] L. Kornaszewski, N. Gayraud, J. M. Stone et al., "Mid-infrared methane detection in a photonic bandgap fiber using a broadband optical parametric oscillator," *Optics Express*, vol. 15, no. 18, pp. 11219–11224, 2007.

[162] A. M. Cubillas, M. Silva-Lopez, J. M. Lazaro, O. M. Conde, M. N. Petrovich, and J. M. Lopez-Higuera, "Methane detection at 1670-nm band using a hollow-core photonic bandgap fiber and a multiline algorithm," *Optics Express*, vol. 15, no. 26, pp. 17570–17576, 2007.

[163] A. M. Cubillas, J. M. Lazaro, M. Silva-Lopez, O. M. Conde, M. N. Petrovich, and J. M. Lopez-Higuera, "Methane sensing at 1300 nm band with hollow-core photonic bandgap fibre as gas cell," *Electronics Letters*, vol. 44, no. 6, pp. 403–405, 2008.

[164] A. M. Cubillas, J. M. Lazaro, O. M. Conde, M. N. Petrovich, and J. M. Lopez-Higuera, "Gas sensor based on photonic crystal fibres in the $2\nu_3$ and $\nu_2 + \nu_3$ vibrational bands of methane," *Sensors*, vol. 9, no. 8, pp. 6261–6272, 2009.

[165] Y. L. Hoo, S. Liu, H. L. Ho, and W. Jin, "Fast response microstructured optical fiber methane sensor with multiple side-openings," *IEEE Photonics Technology Letters*, vol. 22, no. 5, pp. 296–298, 2010.

[166] V. P. Minkovich, D. Monzón-Hernández, J. Villatoro, and G. Badenes, "Microstructured optical fiber coated with thin films for gas and chemical sensing," *Optics Express*, vol. 14, no. 18, pp. 8413–8418, 2006.

[167] J. Villatoro, M. P. Kreuzer, R. Jha et al., "Photonic crystal fiber interferometer for chemical vapor detection with high sensitivity," *Optics Express*, vol. 17, no. 3, pp. 1447–1453, 2009.

[168] Y. L. Hoo, W. Jin, H. L. Ho, and D. N. Wang, "Measurement of gas diffusion coefficient using photonic crystal fiber," *IEEE Photonics Technology Letters*, vol. 15, no. 10, pp. 1434–1436, 2003.

[169] H. Ding, X. Li, J. Cui, S. Dong, and L. Yang, "An all-fiber gas sensing system using hollow-core photonic bandgap fiber as gas cell," *Instrumentation Science and Technology*, vol. 39, no. 1, pp. 78–87, 2011.

[170] T. Ritari, J. Tuominen, H. Ludvigsen et al., "Gas sensing using air-guiding photonic bandgap fibers," *Optics Express*, vol. 12, no. 17, pp. 4080–4087, 2004.

[171] J. Henningsen, J. Hald, and J. C. Petersen, "Saturated absorption in acetylene and hydrogen cyanide in hollow-core photonic bandgap fibers," *Optics Express*, vol. 13, no. 26, pp. 10475–10482, 2005.

[172] M. P. Buric, K. P. Chen, J. Falk, and S. D. Woodruff, "Enhanced spontaneous Raman scattering and gas composition analysis using a photonic crystal fiber," *Applied Optics*, vol. 47, no. 23, pp. 4255–4261, 2008.

[173] M. P. Buric, K. P. Chen, J. Falk, and S. D. Woodruff, "Improved sensitivity gas detection by spontaneous Raman scattering," *Applied Optics*, vol. 48, no. 22, pp. 4424–4429, 2009.

[174] J. P. Parry, B. C. Griffiths, N. Gayraud et al., "Towards practical gas sensing with micro-structured fibres," *Measurement Science and Technology*, vol. 20, no. 7, Article ID 075301, 2009.

[175] H. Lehmann, H. Bartelt, R. Willsch, R. Amezcua-Correa, and J. C. Knight, "In-line gas sensor based on a photonic bandgap fiber with laser-drilled lateral microchannels," *IEEE Sensors Journal*, vol. 11, no. 11, pp. 2926–2931, 2011.

[176] X. Yang, L. Peng, L. Yuan et al., "Oxygen gas optrode based on microstructured polymer optical fiber segment," *Optics Communications*, vol. 284, no. 13, pp. 3462–3466, 2011.

[177] M. T. Myaing, J. Y. Ye, T. B. Norris et al., "Enhanced two-photon biosensing with double-clad photonic crystal fibers," *Optics Letters*, vol. 28, no. 14, pp. 1224–1226, 2003.

[178] X. Yu, D. Yong, H. Zhang et al., "Plasmonic enhanced fluorescence spectroscopy using side-polished microstructured optical fiber," *Sensors and Actuators B*, vol. 160, no. 1, pp. 196–201, 2011.

[179] H. Yan, C. Gu, C. Yang et al., "Hollow core photonic crystal fiber surface-enhanced Raman probe," *Applied Physics Letters*, vol. 89, no. 20, Article ID 204101, 2006.

[180] H. Yan, J. Liu, C. Yang, G. Jin, C. Gu, and L. Hou, "Novel index-guided photonic crystal fiber surface-enhanced Raman scattering probe," *Optics Express*, vol. 16, no. 11, pp. 8300–8305, 2008.

[181] F. M. Cox, A. Argyros, M. C. J. Large, and S. Kalluri, "Surface enhanced Raman scattering in a hollow core microstructured optical fiber," *Optics Express*, vol. 15, no. 21, pp. 13675–13681, 2007.

[182] Y. Zhang, C. Shi, C. Gu, L. Seballos, and J. Z. Zhang, "Liquid core photonic crystal fiber sensor based on surface enhanced Raman scattering," *Applied Physics Letters*, vol. 90, no. 19, Article ID 193504, 2007.

[183] X. Yang, C. Shi, D. Wheeler et al., "High-sensitivity molecular sensing using hollow-core photonic crystal fiber and surface-enhanced Raman scattering," *Journal of the Optical Society of America A*, vol. 27, no. 5, pp. 977–984, 2010.

[184] M. K. Khaing Oo, Y. Han, J. Kanka, S. Sukhishvili, and H. Du, "Structure fits the purpose: photonic crystal fibers for evanescent-field surface-enhanced Raman spectroscopy," *Optics Letters*, vol. 35, no. 4, pp. 466–468, 2010.

[185] J. B. Jensen, L. H. Pedersen, P. E. Hoiby et al., "Photonic crystal fiber based evanescent-wave sensor for detection of biomolecules in aqueous solutions," *Optics Letters*, vol. 29, no. 17, pp. 1974–1976, 2004.

[186] L. Rindorf, P. E. Høiby, J. B. Jensen, L. H. Pedersen, O. Bang, and O. Geschke, "Towards biochips using microstructured optical fiber sensors," *Analytical and Bioanalytical Chemistry*, vol. 385, no. 8, pp. 1370–1375, 2006.

[187] N. Burani and J. Lægsgaard, "Perturbative modeling of bragg-grating-based biosensors in photonic-crystal fibers," *Journal of the Optical Society of America B*, vol. 22, no. 11, pp. 2487–2493, 2005.

[188] L. Rindorf, J. B. Jensen, M. Dufva, L. H. Pedersen, P. E. Høiby, and O. Bang, "Photonic crystal fiber long-period gratings for biochemical sensing," *Optics Express*, vol. 14, no. 18, pp. 8224–8231, 2006.

[189] E. Coscelli, M. Sozzi, F. Poli et al., "Toward a highly specific dna biosensor: PNA-modified suspended-core photonic crystal fibers," *IEEE Journal on Selected Topics in Quantum Electronics*, vol. 16, no. 4, pp. 967–972, 2010.

[190] Y. Ruan, E. P. Schartner, H. Ebendorff-Heidepriem, P. Hoffmann, and T. M. Monro, "Detection of quantum-dot labeled proteins using soft glass microstructured optical fibers," *Optics Express*, vol. 15, no. 26, pp. 17819–17826, 2007.

[191] Y. Ruan, T. C. Foo, S. Warren-Smith et al., "Antibody immobilization within glass microstructured fibers: a route to sensitive and selective biosensors," *Optics Express*, vol. 16, no. 22, pp. 18514–18523, 2008.

[192] S. O. Konorov, A. B. Fedotov, A. M. Zheltikov, and R. B. Miles, "Phase-matched four-wave mixing and sensing of water molecules by coherent anti-stokes Raman scattering in large-core-area hollow photonic-crystal fibers," *Journal of the Optical Society of America B*, vol. 22, no. 9, pp. 2049–2053, 2005.

[193] S. O. Konorov, A. B. Fedotov, L. A. Mel'Nikov, A. V. Shcherbakov, R. B. Miles, and A. M. Zheltikov, "Coherent Raman protocol of biosensing with a hollow photonic-crystal fiber," *Journal of X-ray Science and Technology*, vol. 13, no. 4, pp. 163–169, 2005.

[194] J. Irizar, J. Dinglasan, J. B. Goh et al., "Raman spectroscopy of nanoparticles using hollow-core photonic crystal fibers," *IEEE Journal on Selected Topics in Quantum Electronics*, vol. 14, no. 4, pp. 1214–1222, 2008.

[195] Y. Han, M. K. K. Oo, Y. N. Zhu et al., "Index-guiding liquid-core photonic crystal fiber for solution measurement using normal and surface-enhanced Raman scattering," *Optical Engineering*, vol. 47, no. 4, Article ID 040502, 2008.

[196] Z. Xie, Y. Lu, H. Wei, J. Yan, P. Wang, and H. Ming, "Broad spectral photonic crystal fiber surface enhanced Raman scattering probe," *Applied Physics B*, vol. 95, no. 4, pp. 751–755, 2009.

[197] C. M. B. Cordeiro, M. A. R. Franco, G. Chesini et al., "Microstructured-core optical fibre for evanescent sensing applications," *Optics Express*, vol. 14, no. 26, pp. 13056–13066, 2006.

[198] A. M. Cubillas, M. Schmidt, M. Scharrer et al., "Ultra-low concentration monitoring of catalytic reactions in photonic crystal fiber," *Chemistry*, vol. 18, no. 6, pp. 1586–1590, 2012.

[199] T. G. Euser, J. S. Y. Chen, M. Scharrer, P. S. J. Russell, N. J. Farrer, and P. J. Sadler, "Quantitative broadband chemical sensing in air-suspended solid-core fibers," *Journal of Applied Physics*, vol. 103, no. 10, Article ID 103108, 2008.

[200] X. Yu, Y. Sun, G. B. Ren, P. Shum, N. Q. Ngo, and Y. C. Kwok, "Evanescent field absorption sensor using a pure-silica defected-core photonic crystal fiber," *IEEE Photonics Technology Letters*, vol. 20, no. 5, pp. 336–338, 2008.

[201] C. Wu, B. O. Guan, C. Lu, and H. Y. Tam, "Salinity sensor based on polyimide-coated photonic crystal fiber," *Optics Express*, vol. 19, no. 21, pp. 20003–20008, 2011.

[202] J. Mathew, Y. Semenova, G. Rajan, and G. Farrell, "Humidity sensor based on photonic crystal fibre interferometer," *Electronics Letters*, vol. 46, no. 19, pp. 1341–1343, 2010.
[203] X. H. Yang and L. L. Wang, "Fluorescence ph probe based on microstructured polymer optical fiber," *Optics Express*, vol. 15, no. 25, pp. 16478–16483, 2007.
[204] M. D. Levenson, "Detection of adsorbates on interior surfaces of holey fibers," United States Patent, 2005.
[205] H. Du and S. A. Sukhishvili, "Functionalization of air hole array of phtonic crystal fibers," WIPO and United States Patent, 2006.
[206] Z. Li, M. Tan, S.-Y. Wang, W. Wu, and J. Tang, "Optical sensor and method employing half-core hollow optical waveguide," Unites States Patent, 2010.
[207] A. Khetani, M. Naji, N. Lagali, H. Anis, and R. Munger, "Method for using a photonic crystal fiber as a Raman biosensor," United States Patent, 2010.
[208] C. Gu, Y. Zhang, C. Shi, J. Z. Zhang, and L. Seballos, "Liquid core photonic crystal fiber biosensors using surface enhanced Raman scattering and methods for their use," United States Patent, 2011.
[209] D. U. K. S. Amma, C. Y. Fu, M. Olivo, and K. S. J. Soh, "A photonic crystal fiber sensor," WIPO Patent, 2011.
[210] G. A. S. Sanders, "Photonic crystal fiber sensor," United States Patent, 2010, (Scottsdale, AZ, US).
[211] G. A. Sanders, R. W. Johnson, and S. Yates, "Photonic crystal fiber sensor," Japan, United States and European Patent, 2011.
[212] X. Li, "Photon crystal optical fibre refractivity temperature sensor and measuring systems," China Patent, 2008.
[213] X. Li, "Photon crystal optical fibre fluorescent temperature sensor and measuring systems," China Patent, 2008.
[214] C. Zhao, S. He, X. Dong, and K. Ni, "High-sensitivity temperature sensor based on partial perfusion type HiBi-PCF-FLM (high birefringent photonic crystal fiber loop mirror)," China Patent, 2011.
[215] C. Zhao, Y. Wang, Y. Jin, J. Kang, X. Dong, and S. Jin, "High-birefringence fiber loop mirror (HiBi-FLM) temperature sensor based on photonic crystal fiber-long period grating (PCF-LPG) differential modulation," China Patent, 2011.
[216] C. Zhao, T. Li, X. Dong, W. Qian, and Y. Jin, "Humidity sensor based on tapered and perfused photonic crystal fibers," China Patent, 2011.
[217] C. Zhao, T. Li, X. Dong, W. Qian, and Y. Jin, "Humidity sensor and device based on tapered and injection photonic crystal fiber," China Patent, 2011.
[218] L. An, X. Zhao, and Z. Zheng, "Photonic crystal fiber sensor based on polarization interference," China Patent, 2011.
[219] Z. Weigang, K. Guiyun, J. Long et al., "Photonic crystal fiber fluid sensing device," China Patent, 2005.
[220] T. Wang, W. Ke, and J. Zhao, "Photonic crystal fiber optic liquid level sensor and sensing system formed by same," China Patent, 2011.
[221] C. Zhao, Y. Wang, W. Qian, Y. Qiu, and S. Jin, "HiBi-PCF-FLM (fiber loop mirrors made of highly birefringent photoni crystal fiber) stress sensor based on strength detection differential demodulation and device," China Patent, 2011.
[222] Y. Li, Y. Li, H. Long, and P. Lu, "Current sensor based on photonic crystal fiber grating," China Patent, 2010.
[223] Z. T. Rao, "Hollow photon crystal optical fiber based Fabry-Perot interferometer sensor and its production method," China Patent, 2007.
[224] J. Chen, R. Du, J. Hou et al., "Multi-parameter sensor and measurement system based on photonic crystal fiber," China Patent, 2010.
[225] R. L. Willing, W. P. Kelleher, and S. P. Smith, "Photonic crystal interferometric fiber optical gyroscope system," United States Patent, 2004.
[226] M. J. F. Digonnet, H. K. Kim, S. Blin, V. Dangui, and G. S. Kino, "Optical Sensor utilizing hollow-core photonic bandgap fiber with low phase thermal constant," United States Patent, 2008.